Vector Boson Scattering results in CMS

Costanza Carrivale
(Università degli Studi di Perugia, INFN Perugia)
on behalf of the CMS Collaboration

31st International Workshop on Deep Inelastic Scattering, 9 April 2024

Vector Boson Scattering at LHC

Diagrams in which two Vector Bosons interact, giving either one or two Vector Bosons in the final state, are among the rarest processes measured.

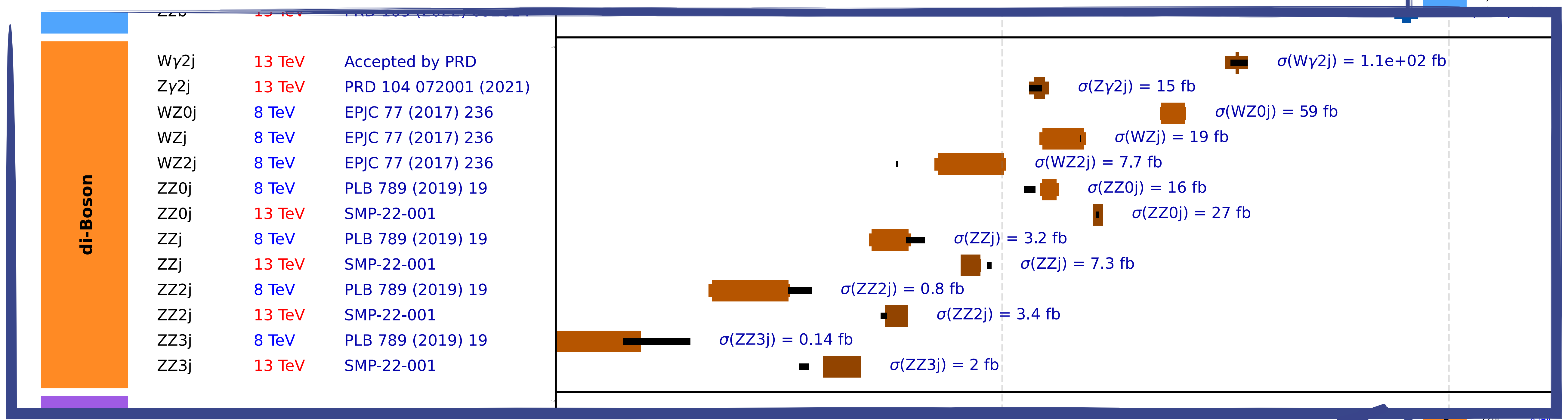

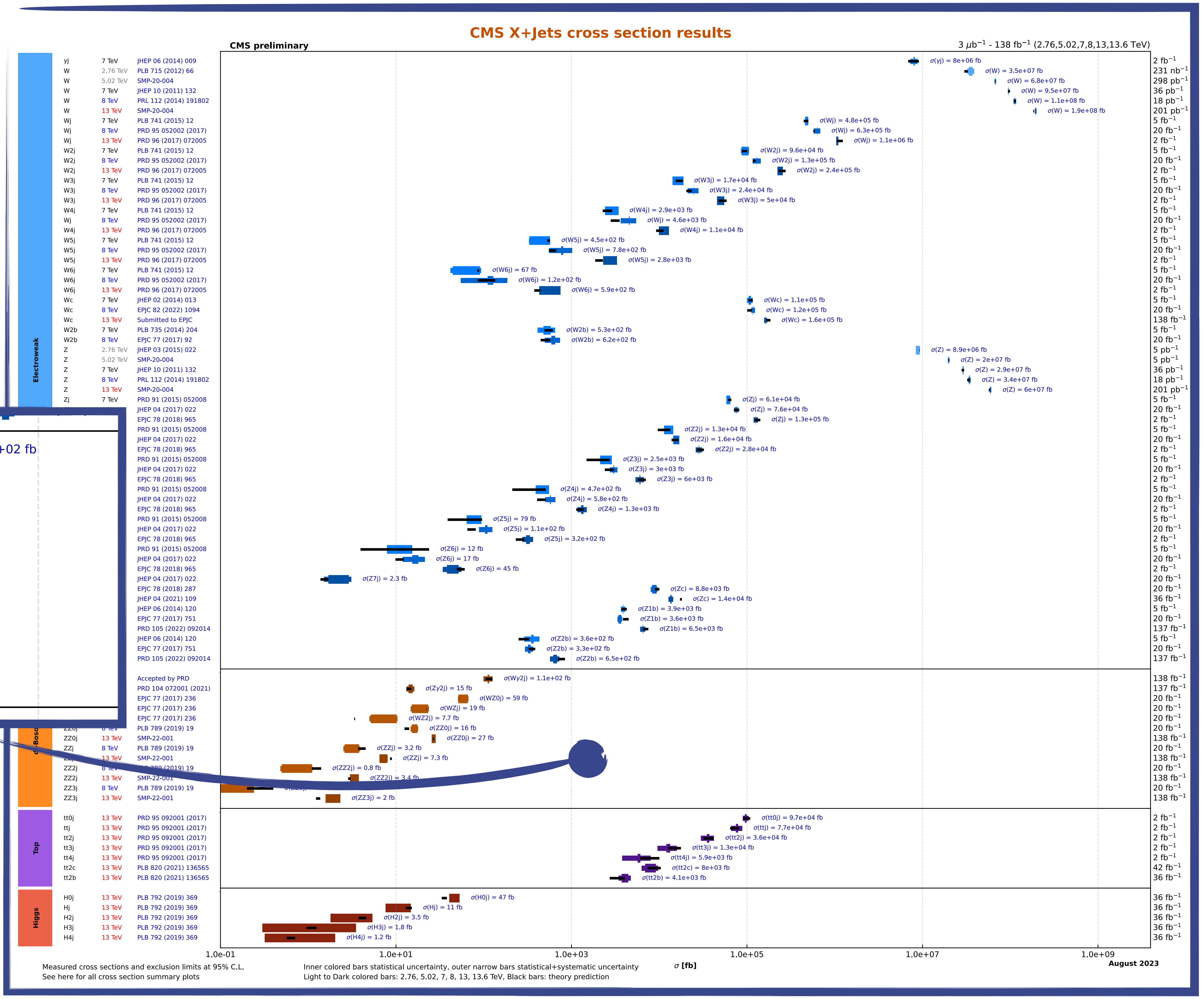

Why is VBS so charming?

- EW sector of the Standard Model is based on $SU(2)_L \otimes SU(1)_Y$ symmetry group. The non-abelian nature of the group results in self-interaction of the gauge bosons (triple and quartic gauge couplings, **TGCs and QGCs**). VBS processes exhibit both types of interaction.

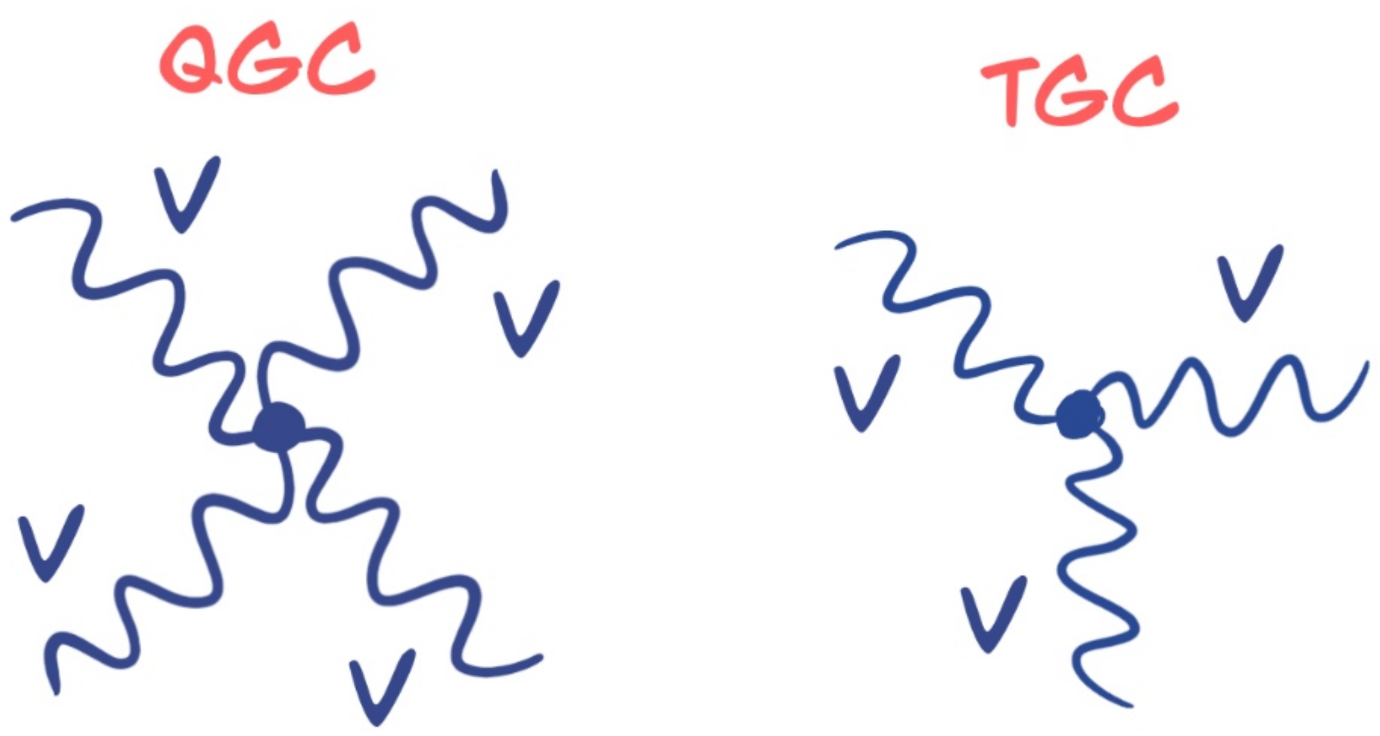

- VBS processes are strictly related to **unitarity violation** in SM and precise measurements of VBS can probe the nature of the Higgs sector

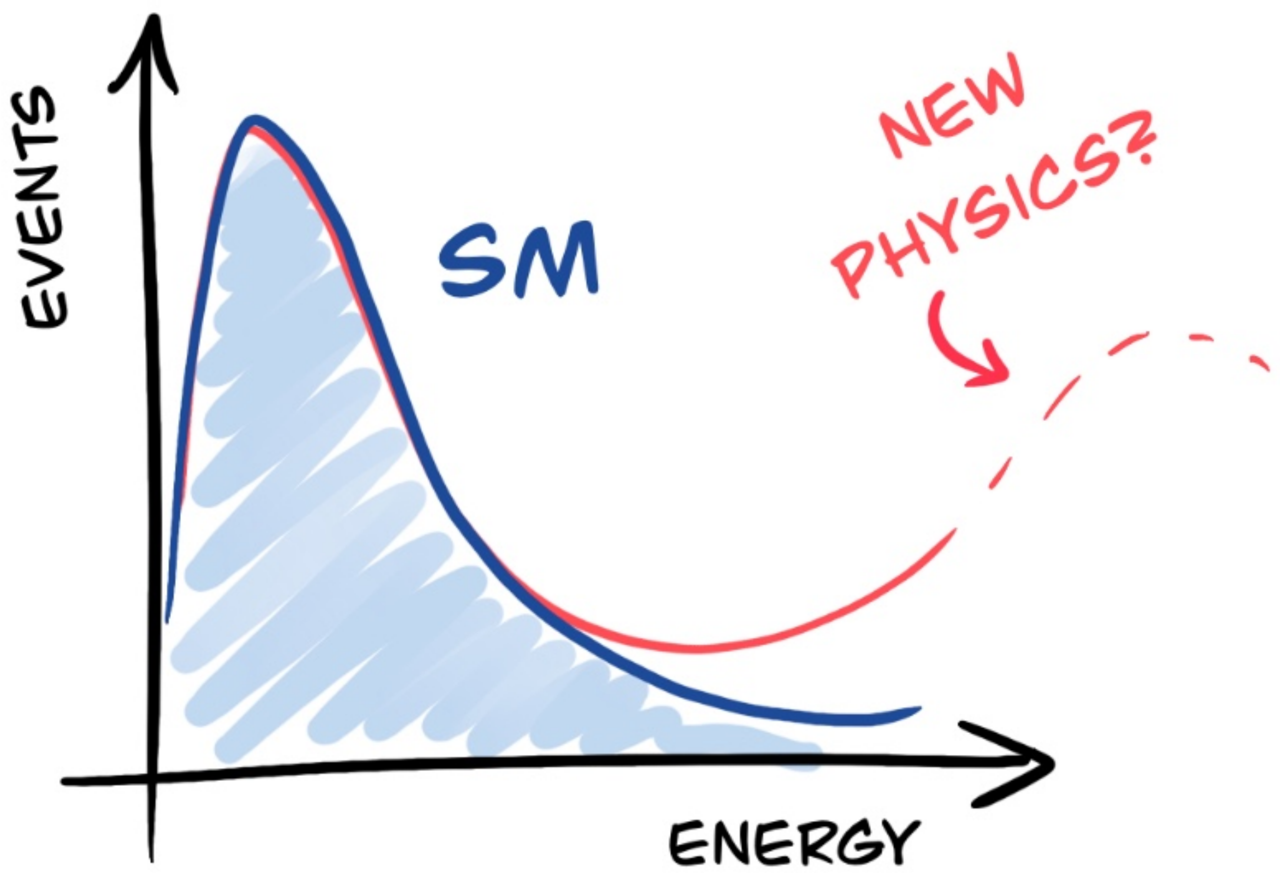

- Powerful instrument to search for **effects beyond the SM** using model-independent approaches

VBS topology in proton-proton collisions

VBS contributes to EW-induced diboson production at tree level $\mathcal{O}(\alpha^4)$.

At LHC interactions from VBS are characterized by:

- Presence of two vector bosons in the central part of the detector;
- Two forward-backward jets with high dijet invariant mass and large pseudorapidity separation.

Typical observables in VBS measurements at LHC are cross sections in detector fiducial regions.

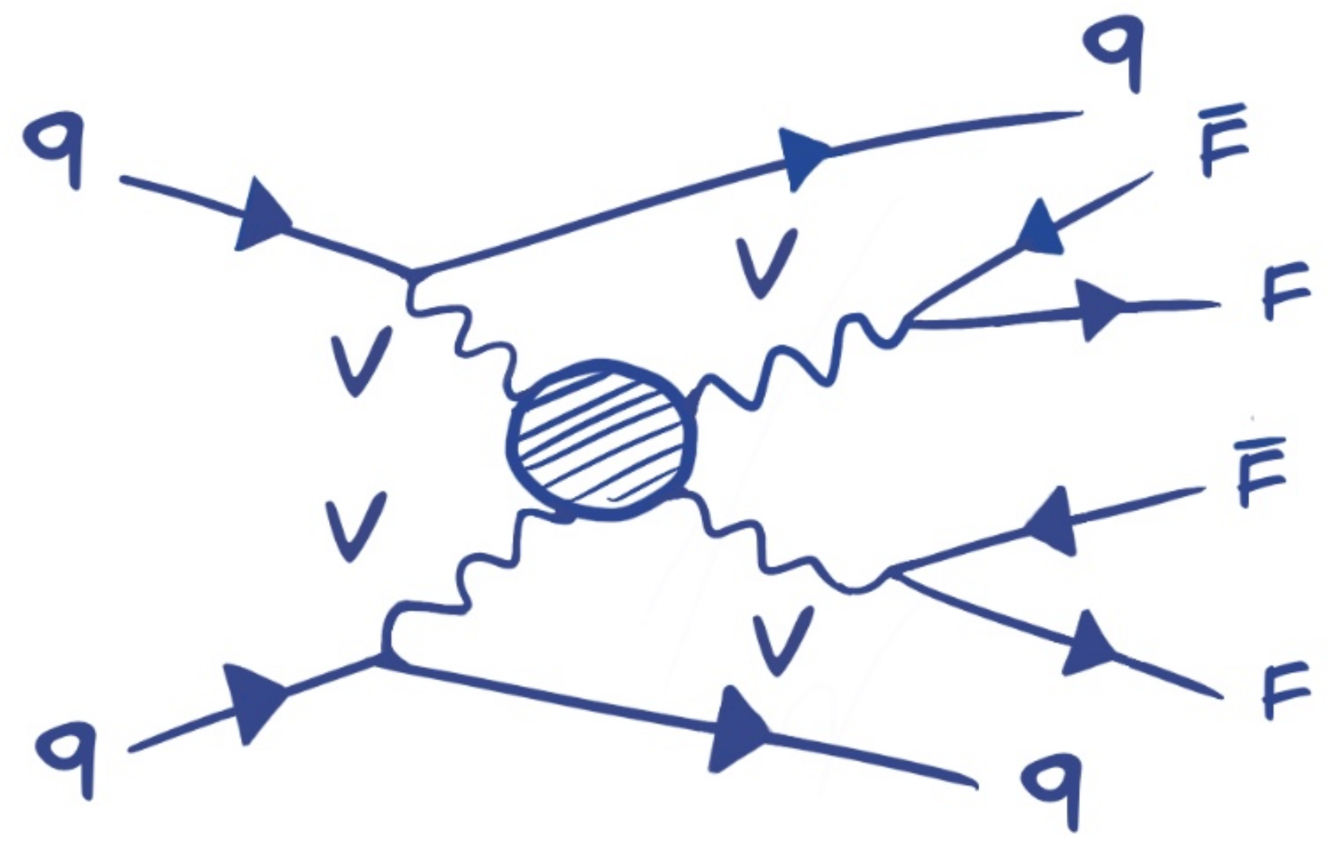

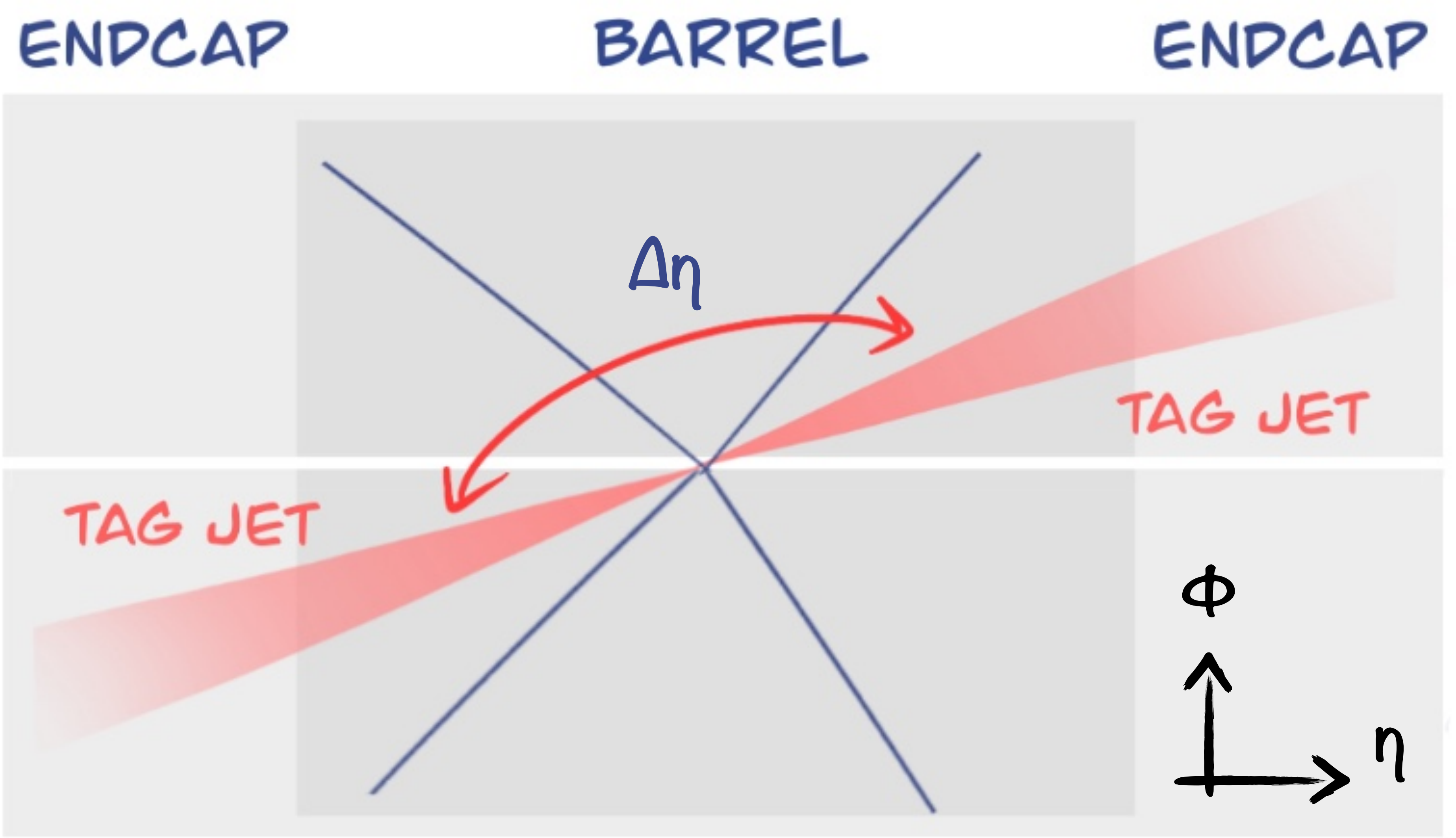

Recent results in CMS

CMS results for VBS processes at $\sqrt{s} = 13$ TeV and integrated luminosity of 138 fb^{-1}

2020

Polarized ssWW
Production xsec of longitudinally polarized W
Phys. Lett. B 812 (2020) 136018

2021

Zγjj
Observation and differential xsec, limits on EFT@dim8
Phys. Lett. B 812 (2021) 135992

ZZ to 4Ljj
Observation and fiducial xsec, limits on EFT@dim8
Phys. Lett. B 812 (2021) 135992

2022

Semi-leptonic WVjj
Observation and xsec
Phys. Lett. B 834 (2022) 137438

Fully-leptonic ssWW with hadr. tau
Xsec measurement, 2D limits on EFT@dim6+dim8 (?)
CMS-PAS-SMP-22-008

2023

Fully-leptonic osWW
Observation and xsec
Phys. Lett. B 841 (2023) 137495

Wγjj
Observation and differential xsec, limits on EFT@dim8
Phys.Rev.D 108 (2023) 032017

2024

Opposite-sign WW VBS

EWK production of a pair of opposite-sign Ws and two jets, with both W decaying leptonically.

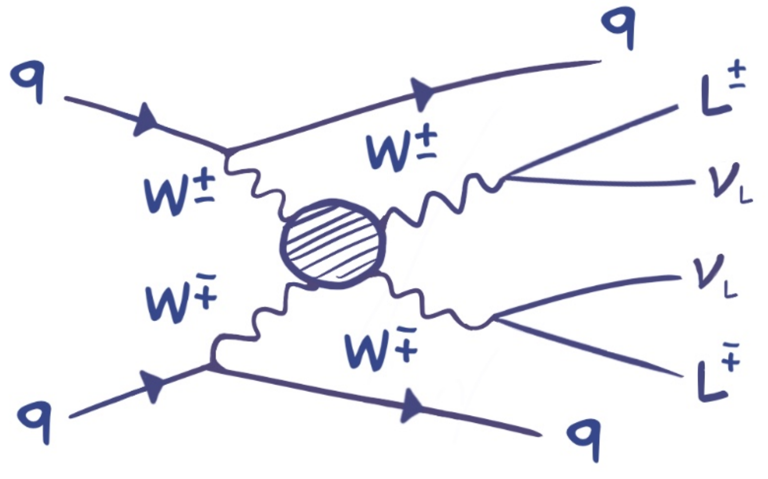

The analysis selects final states with two OS leptons: e^+e^-, $\mu^+\mu^-$, $e^\pm\mu^\mp$.
Sources of background:

- Top pair production makes the measurement quite challenging. Studied in a dedicated CR (~95% pure sample $t\bar{t}$)
- Drell Yan is one of the leading backgrounds in ee and $\mu\mu$ categories (~91% wrt 64% in $e\mu$), comes from different sources
- Non-prompt (data driven)
- QCD-induced WW, Higgs, multiboson

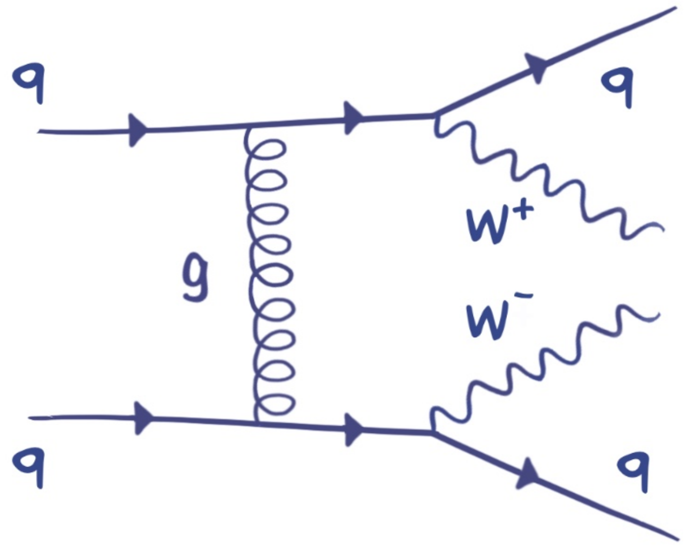

Events where at least one jet comes from a pileup vertex $|\Delta\eta_{jj}| > 5$

Events where both jets are generated in hard interaction $|\Delta\eta_{jj}| < 5$

$\tau\tau$

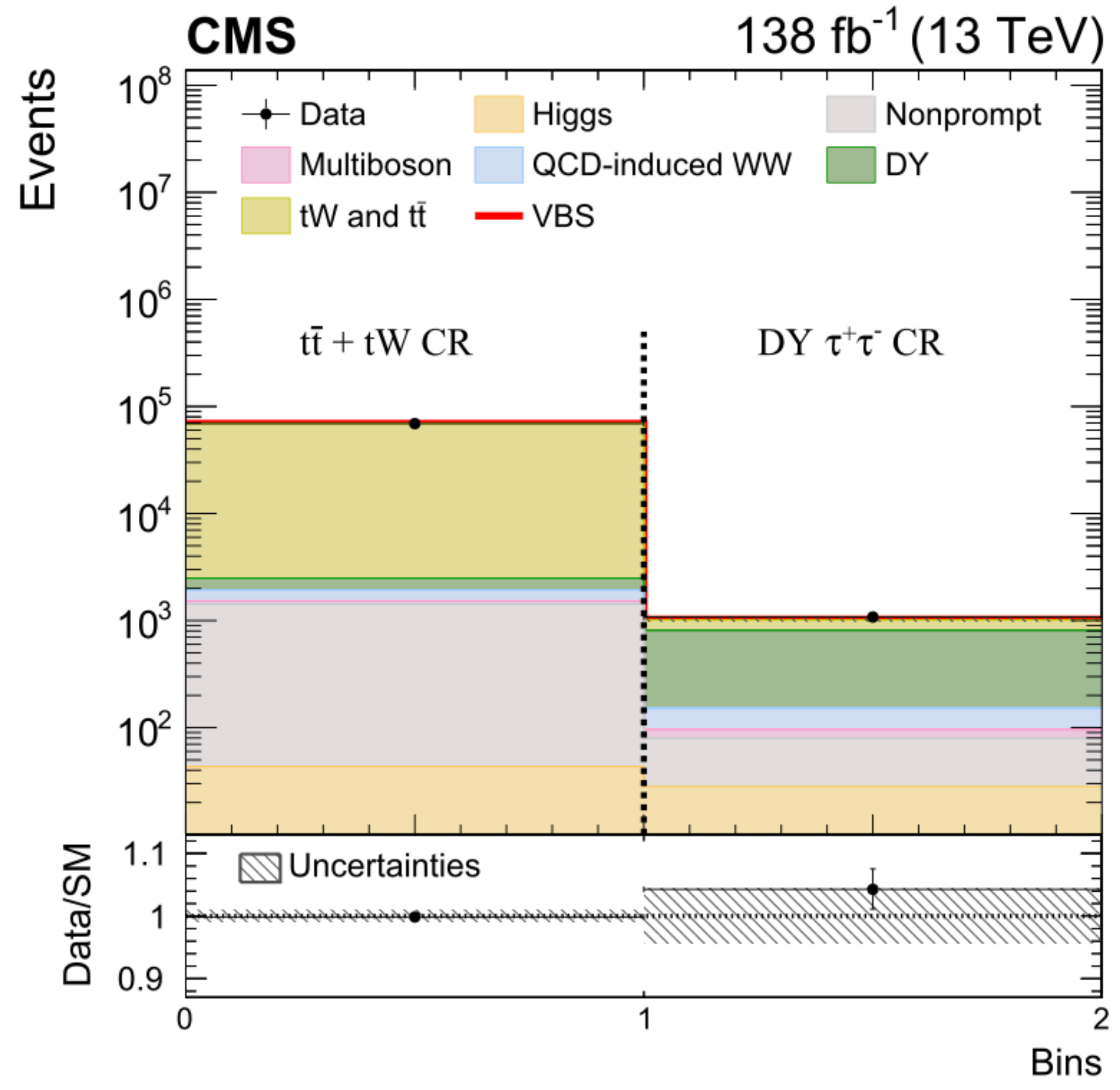

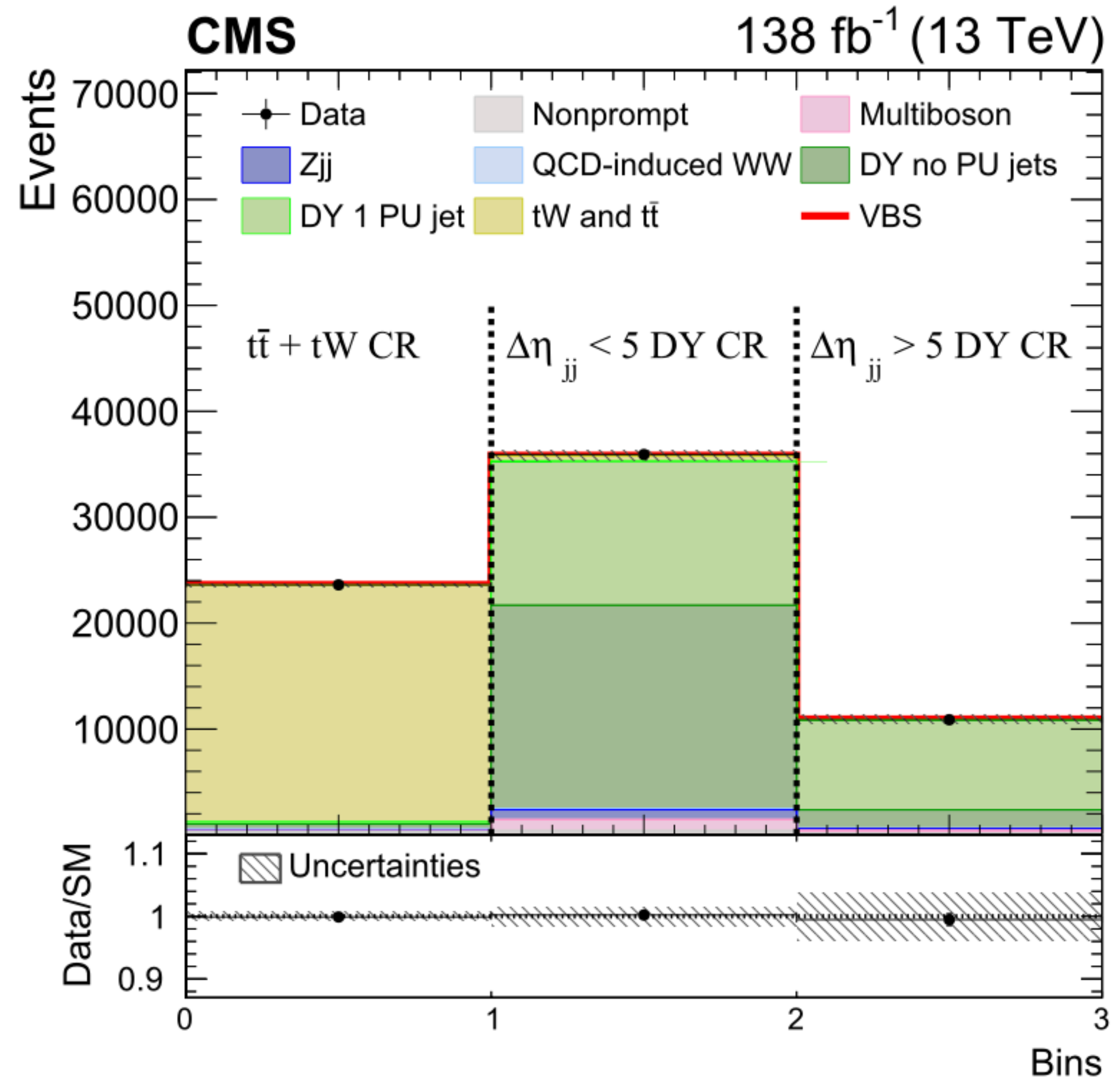

Opposite-sign WW VBS

SR is split in two regions to optimize the signal significance, based on centrality of dilepton system with respect to the tagging jets, quantified by Zeppenfeld variable $Z_{ll} = \frac{1}{2}\,|\eta_{l1} + \eta_{l2} - (\eta_{j1} + \eta_{j2})\,|$.

All categories are fit to data using a maximun likelihood fit and different discriminating variables:

- A feed-forward deep neural network (DNN) for $e\mu$
- Different variables in different regions for ee and $\mu\mu$:

$$\text{n. events} \begin{cases} mjj \in [300;500] \text{ and } |\Delta\eta_{jj}| \in [2.5;3.5] & \text{bin 1} \\ mjj > 500 \text{ and } |\Delta\eta_{jj}| \in [2.5;3.5] & \text{bin 2} \\ mjj \in [300;500] \text{ and } |\Delta\eta_{jj}| > 3.5 & \text{bin 3} \end{cases}$$

$$m_{jj} \quad mjj > 500 \text{ and } |\Delta\eta_{jj}| > 3.5 \quad \text{bins 4-8}$$

The observed (expected) significance is 5.6 (5.2) σ.

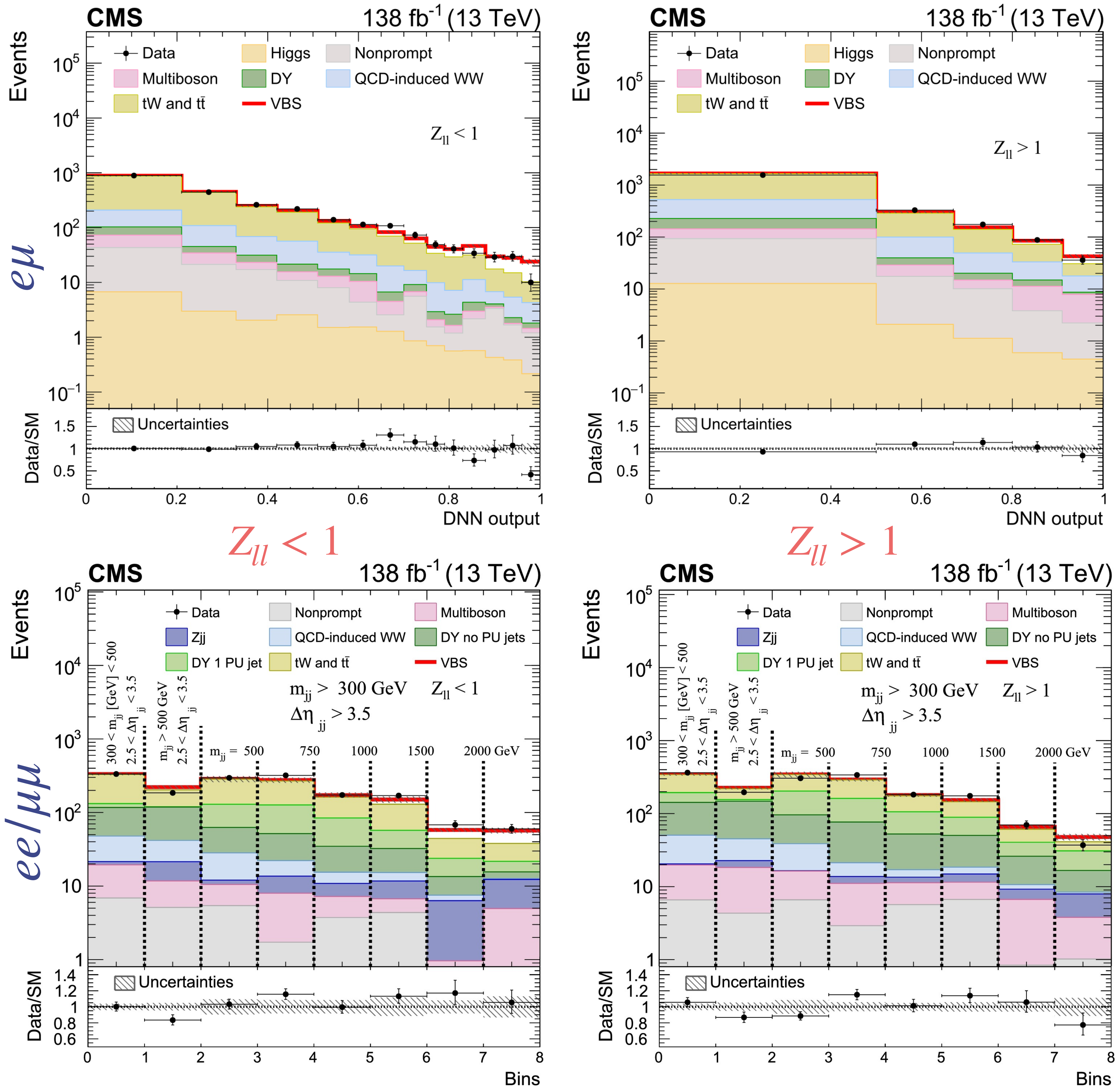

Opposite-sign WW VBS

EW osWW production cross section is measured in two different fiducial volumes:

- Inclusive volume (no tau veto, outgoing partons with $p_T > 10$ GeV and $m_{qq'} > 100$ GeV): $\sigma_{obs} = 99 \pm 20$ **fb**, $\sigma_{exp} = 89 \pm 5$ **(scale) fb**
- Fiducial volume similar to reconstructed SR: $\sigma_{obs} = 10.2 \pm 2.0$ **fb**, $\sigma_{exp} = 9.1 \pm 0.6$ **(scale) fb**

Objects	Requirements
Leptons	$e\mu$, ee, $\mu\mu$ (not from τ decay), opposite charge $p_T^{\text{dressed}\,\ell} = p_T^{\ell} + \sum_i p_T^{\gamma_i}$ if $\Delta R(\ell, \gamma_i) < 0.1$ $p_T^{\ell_1} > 25\,\text{GeV}$, $p_T^{\ell_2} > 13\,\text{GeV}$, $p_T^{\ell_3} < 10\,\text{GeV}$ $\lvert\eta\rvert < 2.5$ $p_T^{\ell\ell} > 30\,\text{GeV}$, $m_{\ell\ell} > 50\,\text{GeV}$
Jets	$p_T^{j} > 30\,\text{GeV}$ $\Delta R(j, \ell) > 0.4$ At least 2 jets, no b jets $\lvert\eta\rvert < 4.7$ $m_{jj} > 300\,\text{GeV}$, $\lvert\Delta\eta_{jj}\rvert > 2.5$
p_T^{miss}	$p_T^{miss} > 20\,\text{GeV}$

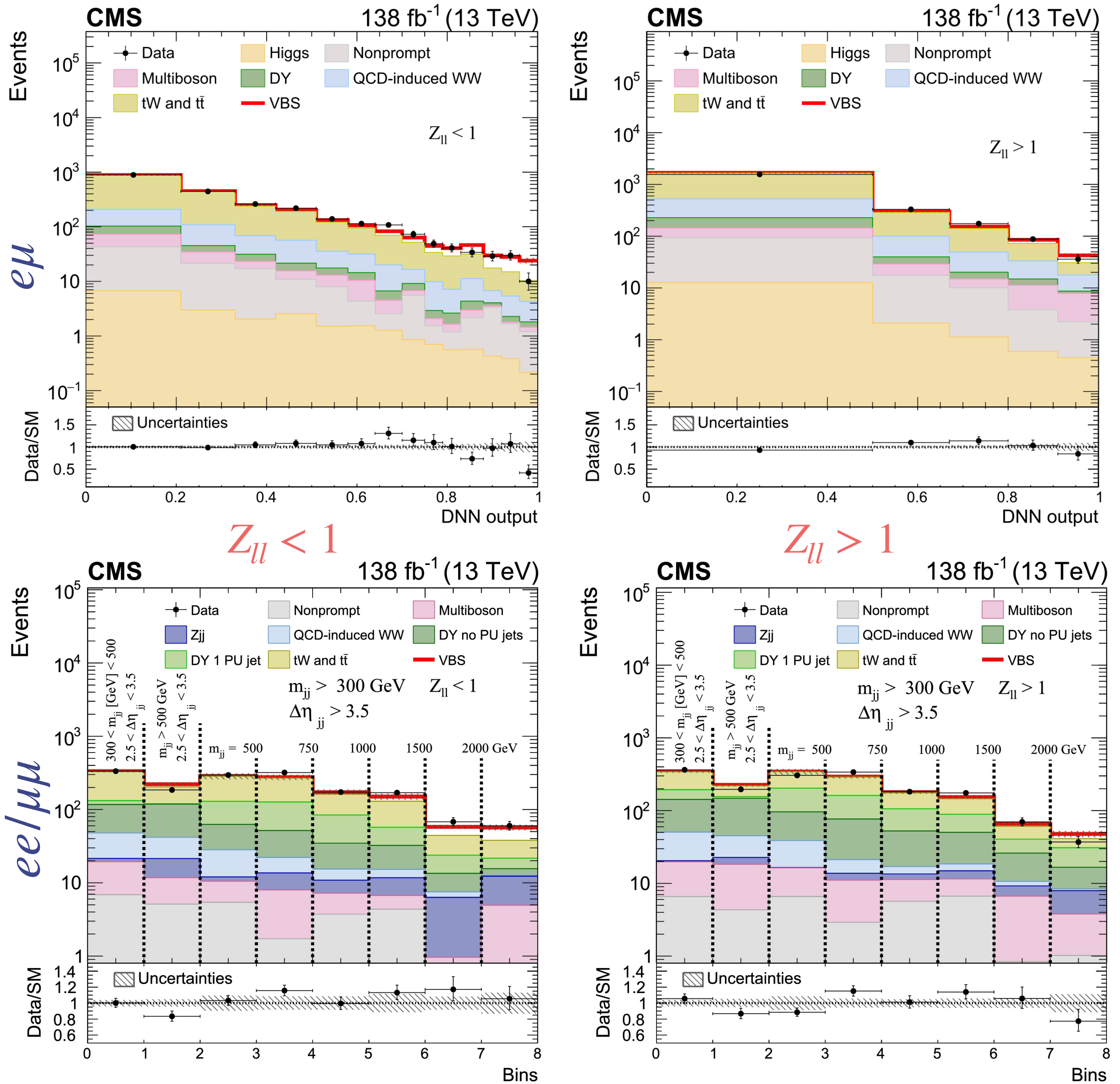

EWK production of $W\gamma$ +2jets

EWK production of W, γ and two jets, with W boson decaying in the leptonic channel.

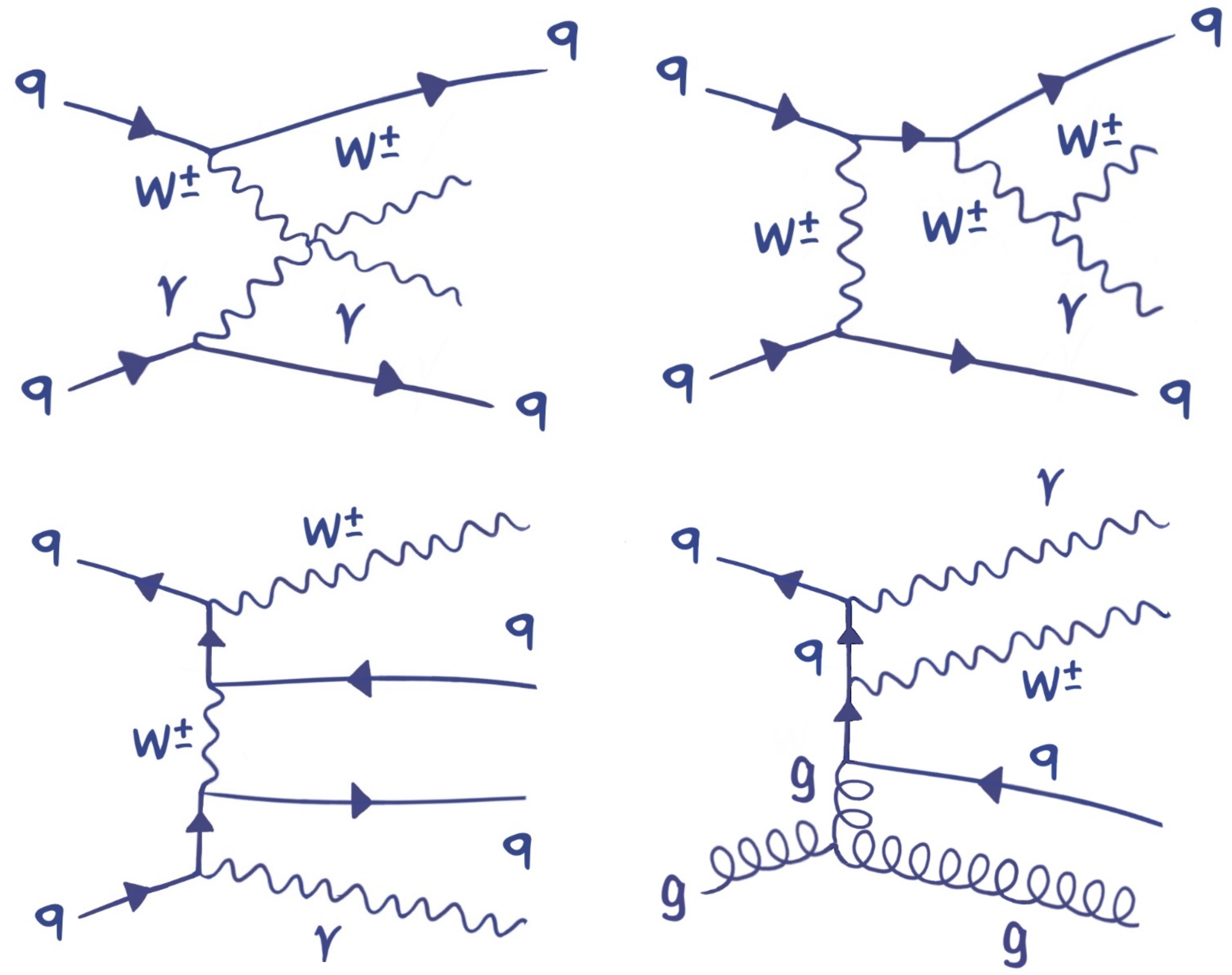

Main backgrounds sources are:

- W+jets
- Top quark processes with jet misidentified as photon
- Top, VV, $Z\gamma$

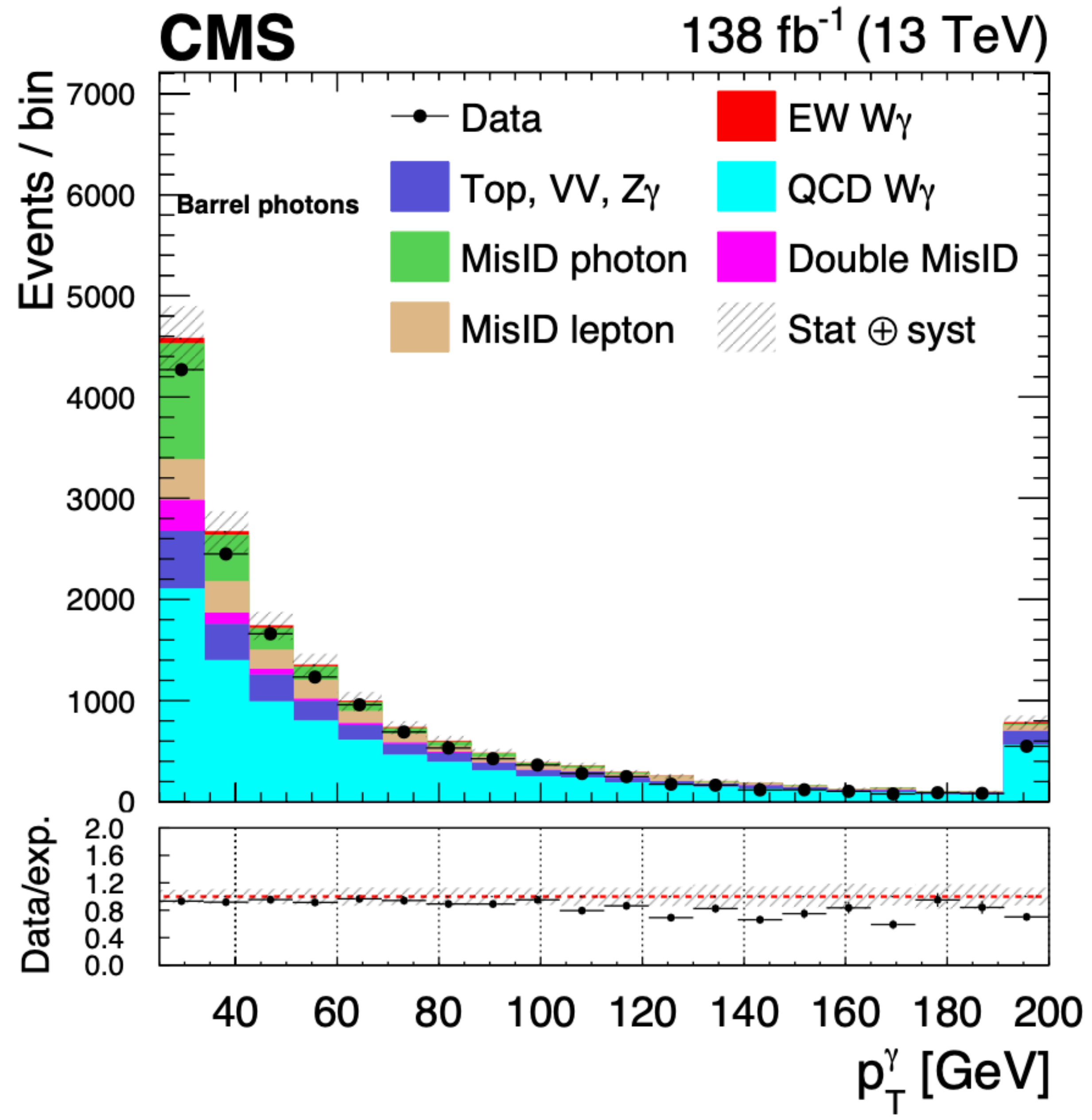

Scale factors for non-prompt photons are extrapolated in a loose-γ Control Region and are applied in the Signal Region. Discrimination relies on the photon $\sigma_{\eta\eta}$, an observable that quantifies the lateral extension of the shower.

EWK production of Wγ +2jets

- Measurement of EW Wγ production rate is extracted using a binned likelihood fit to a 2D distribution in $m_{l\gamma}$ and m_{jj}. The observed (expected) significance is **6.0 (6.8) σ**.
- The purely EW ($\mu_{QCD} = 1$) and EW+QCD W fiducial cross section is measured in a fiducial region as $\sigma^{fid} = \sigma_g \hat{\mu} \alpha$, where σ_g is the cross section calculated with MadGraph5 at LO in QCD.

Signal	$\mu = \sigma_{OBS}/\sigma_{SM}$	Cross Section [fb]
EWK Wγ	$0.88^{+0.19}_{-0.18}$	$23.5 \pm 2.8(\text{stat})^{+1.9}_{-1.7}(\text{th})^{+3.5}_{-3.4}(\text{stat})$
EWK+QCD Wγ	$0.98^{+0.12}_{-0.11}$	$113 \pm 2.0(\text{stat})^{+2.5}_{-2.3}(\text{th})^{+13}_{-13}(\text{stat})$

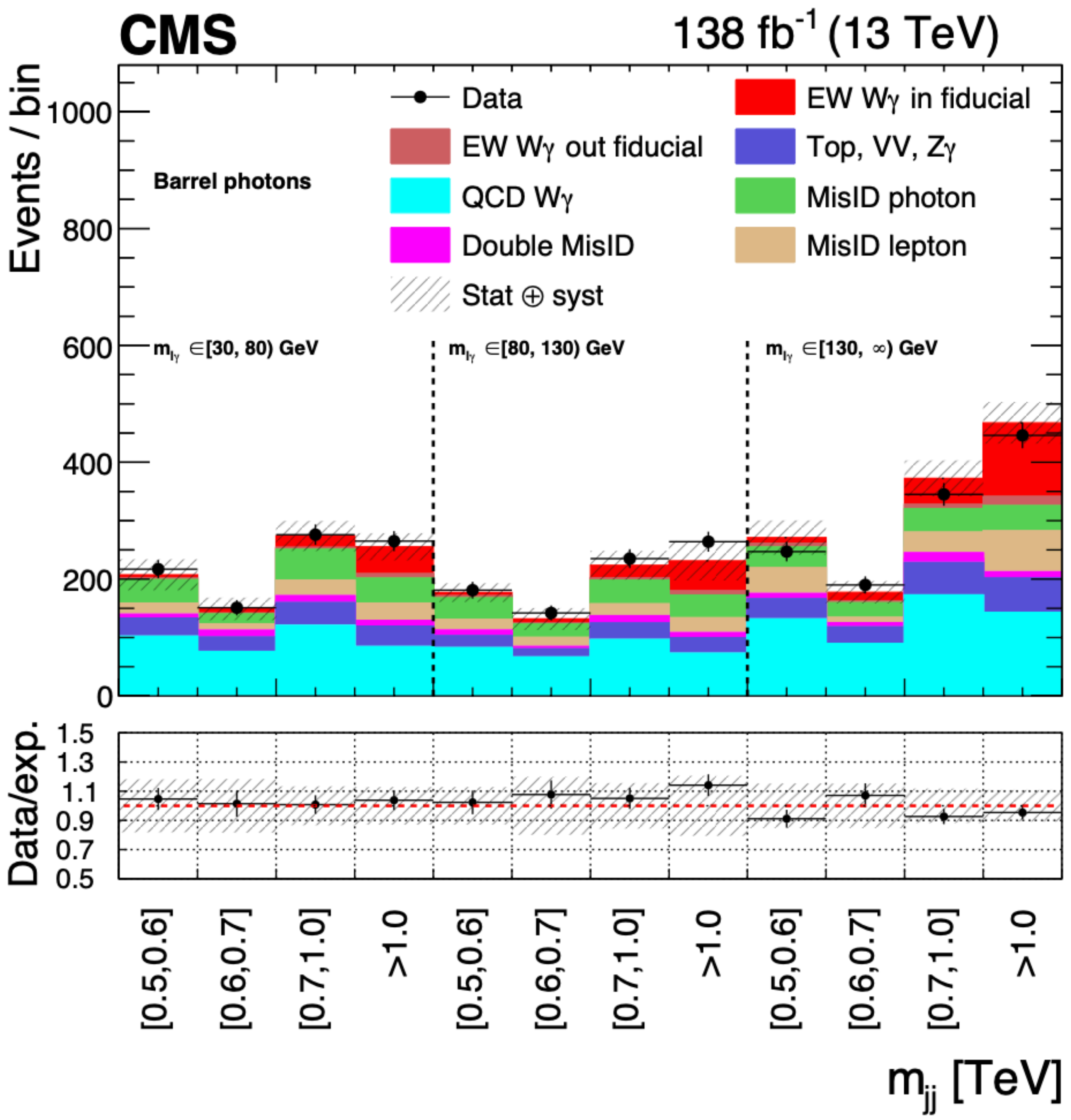

All the results are in agreement with SM predictions.

EWK production of Wγ +2jets

EFT interpretation

Constraints on anomalous quartic gauge couplings for EFT@dim8 operators are extracted @95%CL via likelihood scan approach.

- One operator at the time (other EFT couplings set to zero)
- $m_{W\gamma}$ distribution built in the VBS phase-space region to enhance sensitivity to aQGC

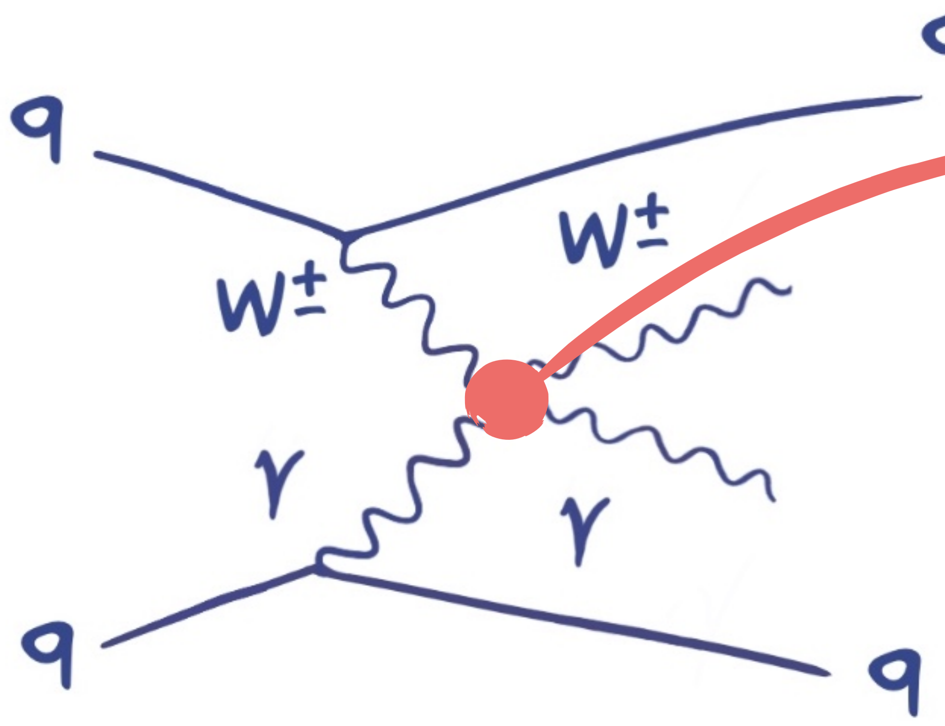

$$\mathcal{L}_{\rm EFT} = \mathcal{L}_{\rm SM} + \sum_i \frac{f_i^{(8)}}{\Lambda^4}\mathcal{O}_i^{(8)} + \ldots$$

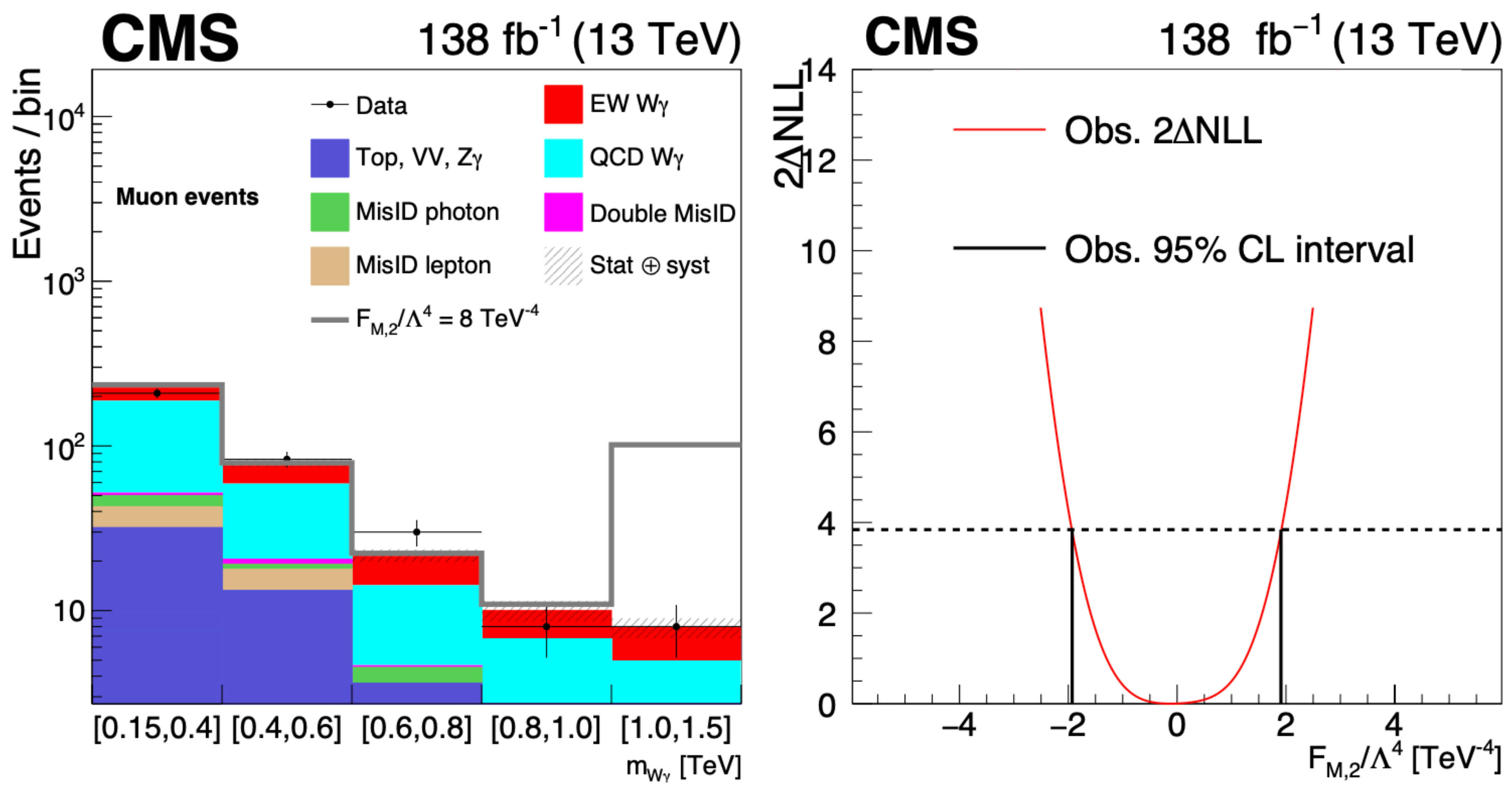

Expected limit	Observed limit	$U_{\rm bound}$
$-5.1 < f_{M,0}/\Lambda^4 < 5.1$	$-5.6 < f_{M,0}/\Lambda^4 < 5.5$	1.7
$-7.1 < f_{M,1}/\Lambda^4 < 7.4$	$-7.8 < f_{M,1}/\Lambda^4 < 8.1$	2.1
$-1.8 < f_{M,2}/\Lambda^4 < 1.8$	$-1.9 < f_{M,2}/\Lambda^4 < 1.9$	2.0
$-2.5 < f_{M,3}/\Lambda^4 < 2.5$	$-2.7 < f_{M,3}/\Lambda^4 < 2.7$	2.7
$-3.3 < f_{M,4}/\Lambda^4 < 3.3$	$-3.7 < f_{M,4}/\Lambda^4 < 3.6$	2.3
$-3.4 < f_{M,5}/\Lambda^4 < 3.6$	$-3.9 < f_{M,5}/\Lambda^4 < 3.9$	2.7
$-13 < f_{M,7}/\Lambda^4 < 13$	$-14 < f_{M,7}/\Lambda^4 < 14$	2.2
$-0.43 < f_{T,0}/\Lambda^4 < 0.51$	$-0.47 < f_{T,0}/\Lambda^4 < 0.51$	1.9
$-0.27 < f_{T,1}/\Lambda^4 < 0.31$	$-0.31 < f_{T,1}/\Lambda^4 < 0.34$	2.5
$-0.72 < f_{T,2}/\Lambda^4 < 0.92$	$-0.85 < f_{T,2}/\Lambda^4 < 1.0$	2.3
$-0.29 < f_{T,5}/\Lambda^4 < 0.31$	$-0.31 < f_{T,5}/\Lambda^4 < 0.33$	2.6
$-0.23 < f_{T,6}/\Lambda^4 < 0.25$	$-0.25 < f_{T,6}/\Lambda^4 < 0.27$	2.9
$-0.60 < f_{T,7}/\Lambda^4 < 0.68$	$-0.67 < f_{T,7}/\Lambda^4 < 0.73$	3.1

Most stringent limits to date on several aQGC parameters.

Same-sign WW with hadronic tau

EWK production of same-sign W boson pairs with a hadronically decaying τ in the final state.

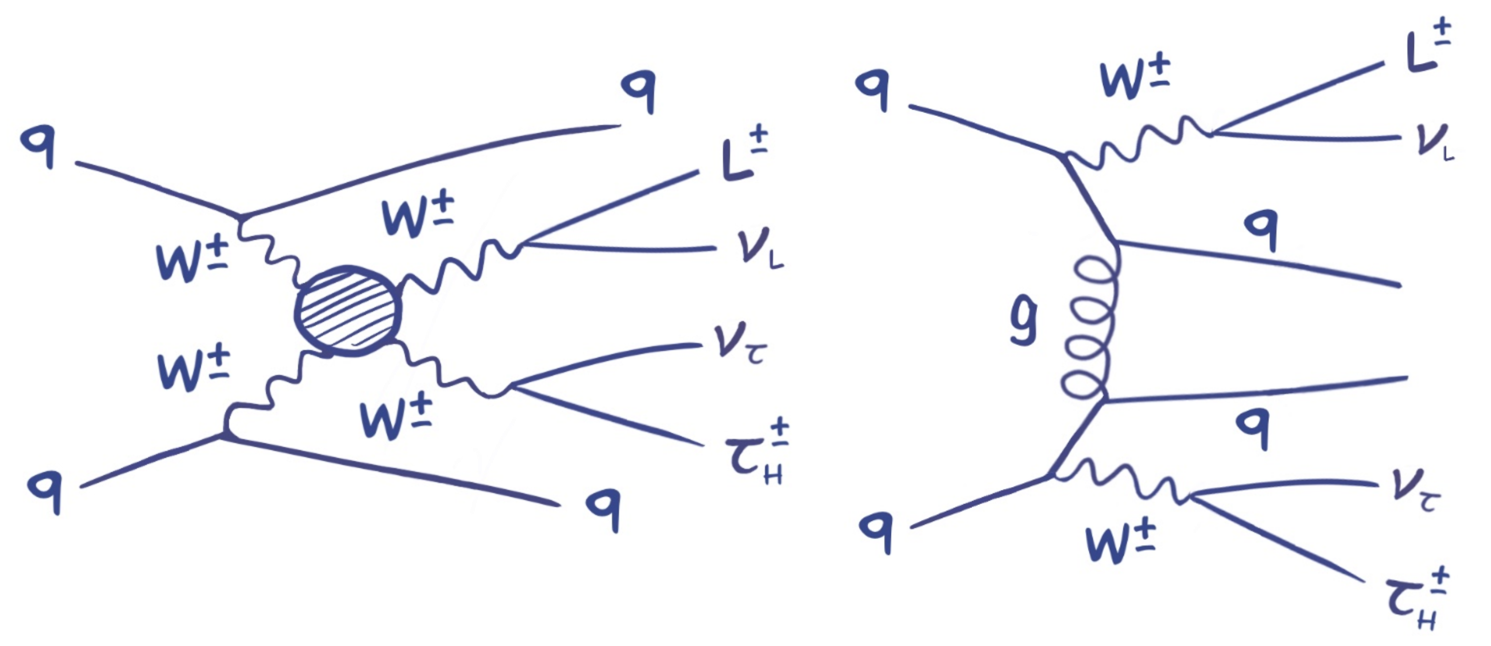

Same-sign WW is the golden channel for VBS studies due to good separation between EWK and QCD components and full availability of NLO corrections.

Main backgrounds sources in SR are:

- events containing nonprompt leptons from QCD-mediated multijet, W+jets, hadr. and semi-leptonic tt (**95%**)
- Z/γ^* + jets (2%)
- Dileptonic tt production (1%)

QCD-enriched region | Non-prompt CR

Opposite-sign CR

tt CR

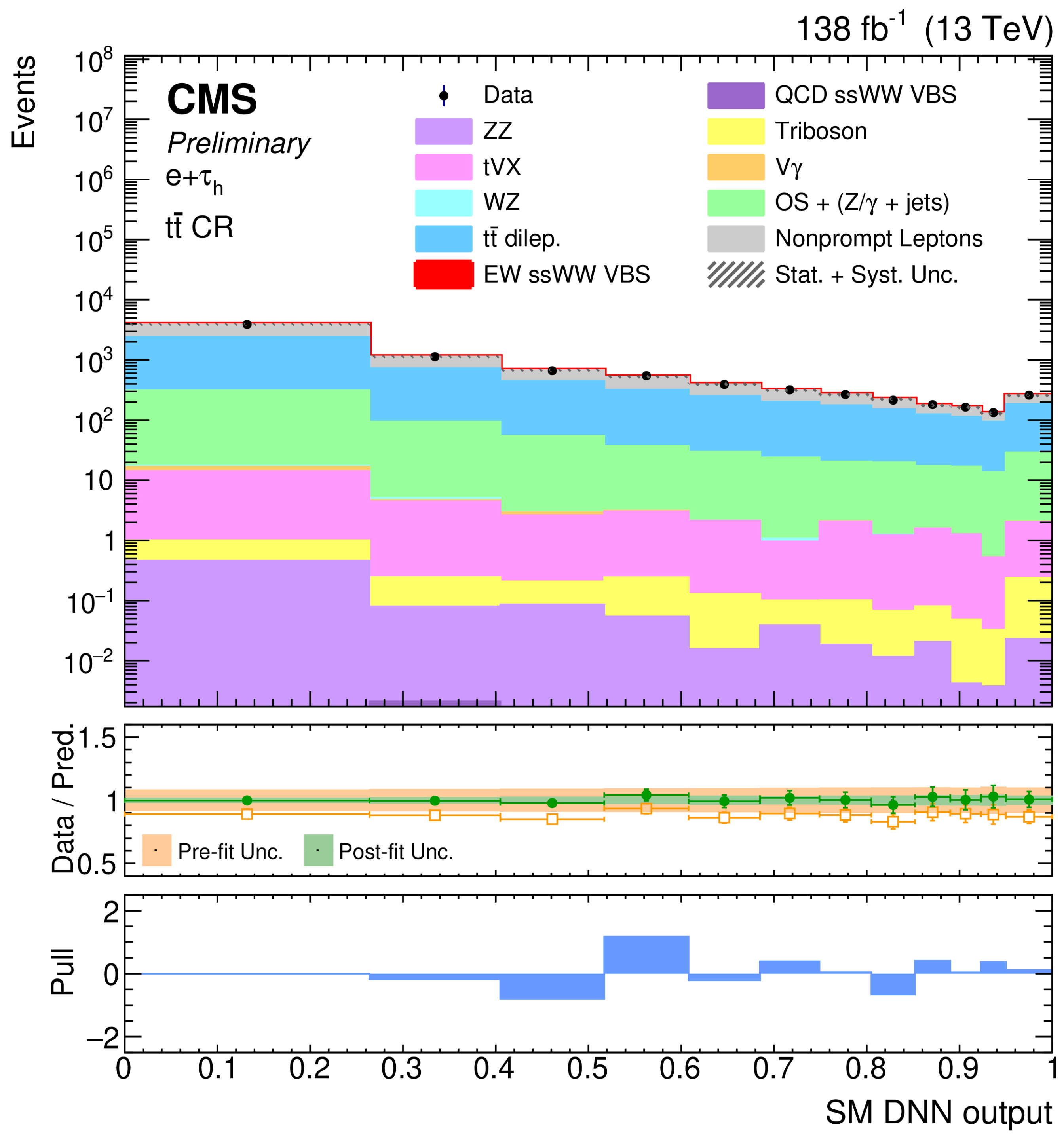

Same-sign WW with hadronic tau

- 9 significant observables are combined in a single ML discriminator (DNN) to separate signal and background. Two dedicated transverse masses are defined:

$$M_{1T}^2 = \left(\sqrt{M_{\tau l}^2 + p_T^{\tau l 2}} + p_T^{\text{miss}}\right)^2 - |\vec{p}_T^{\tau l} + \vec{p}_T|^2$$

$$M_{o1}^2 = \left(p_T^{\tau} + p_T^{l} + p_T\right)^2 - |\vec{p}_T^{\tau l} + \vec{p}_T^{l} + \vec{p}_T|^2$$

- Measurement of purely EW ssWW signal strenght ($\mu_{\text{QCD}} = 1$) and EWK+QCD ssWW signal strenght:

Signal	$\mu = \sigma_{OBS}/\sigma_{SM}$	Significance $[\sigma]$
EWK ssWW	$1.44^{+0.63}_{-0.56}$	2.7 (1.9 exp)
EWK+QCD ssWW	$1.43^{+0.60}_{-0.54}$	2.9 (2.0 exp)

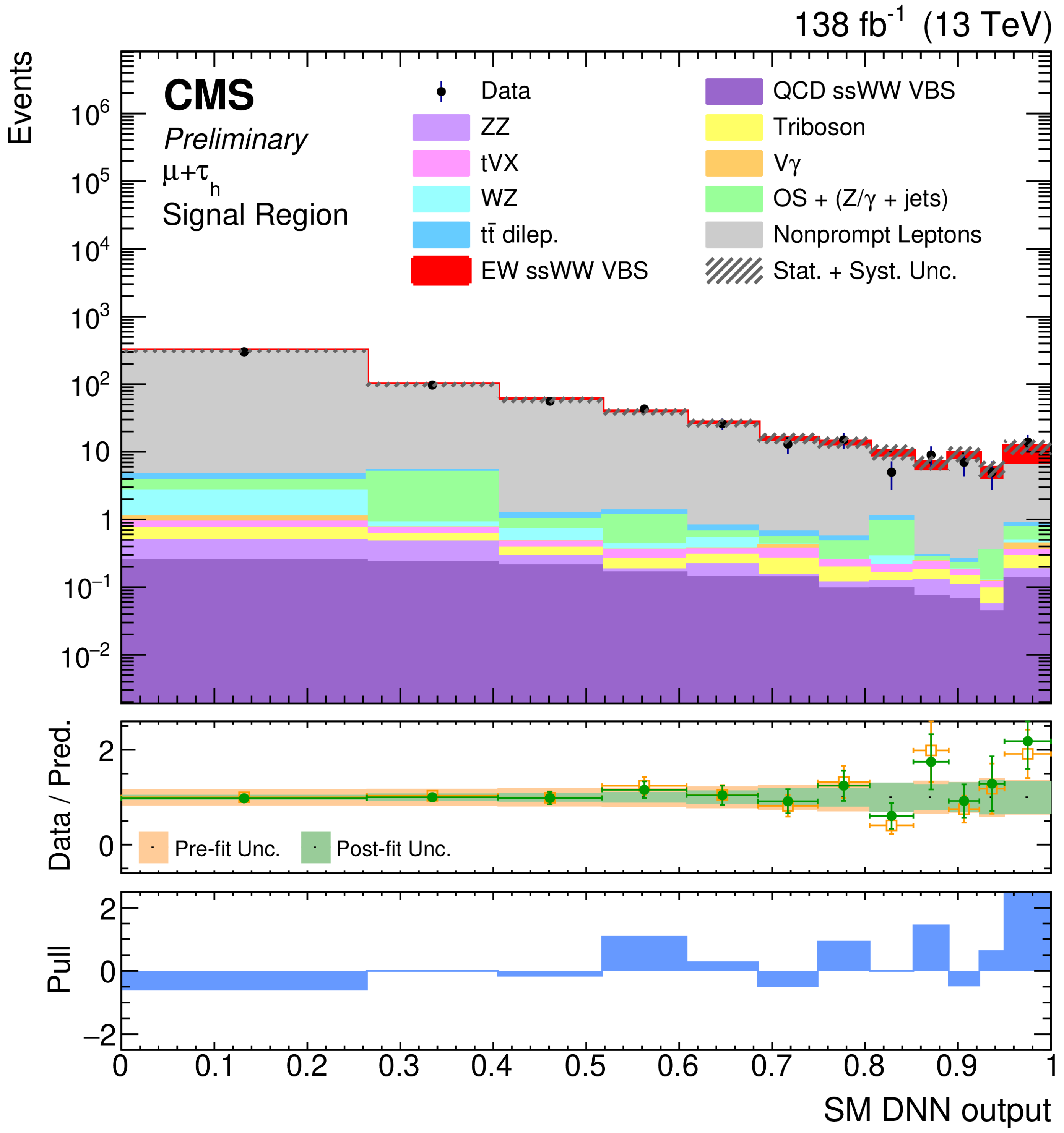

Same-sign WW with hadronic tau

EFT interpretation

Constraints on bosonic dim6 and dim8 EFT Wilson coefficients are derived via likelihood scan approach. Both 1D and 2D limits are extrapolated.

First analysis considering pairs of different dimension operators in 2D scan.

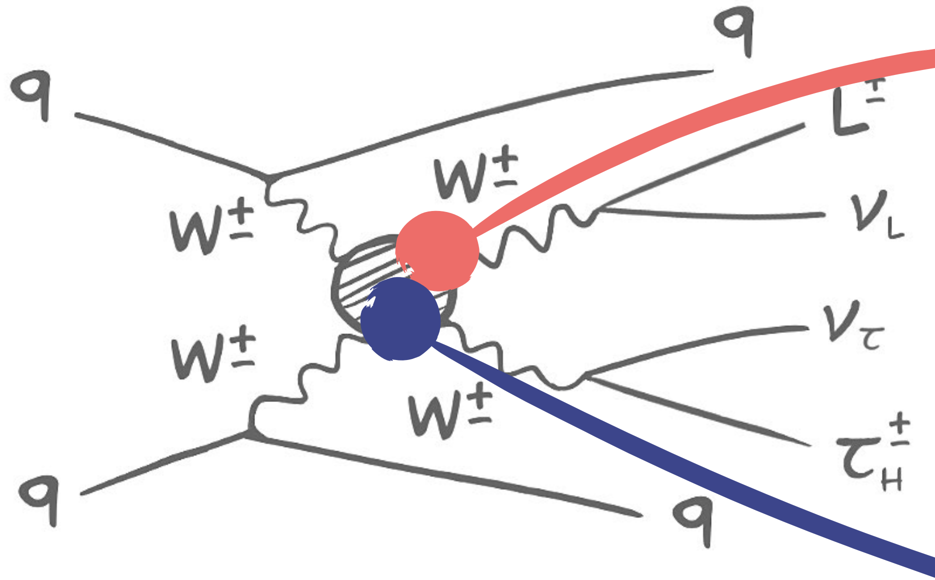

$$\mathcal{L}_{\mathrm{EFT}} = \mathcal{L}_{\mathrm{SM}} + \sum_i \frac{c_i^{(6)}}{\Lambda^2}\mathcal{O}_i^{(6)} + \sum_i \frac{f_i^{(8)}}{\Lambda^4}\mathcal{O}_i^{(8)} + \ldots$$

- 1D limits consider one operator at the time
- 2D limits couple operators that give similar contributions to the $WW \to WW$ scattering amplitude and that have a similar ratio between quadratic and linear terms.

dimension 6

$$\mathcal{O}_W = \epsilon^{ijk} W_\mu^{\nu i} W_\nu^{\rho j} W_\rho^{\mu k}$$
$$\mathcal{O}_{\varphi\Box} = (\varphi^\dagger\varphi)\Box(\varphi^\dagger\varphi)$$
$$\mathcal{O}_{\varphi D} = (\varphi^\dagger D^\mu \varphi) * (\varphi^\dagger D_\mu \varphi)$$
$$\mathcal{O}_{\varphi W} = \varphi^\dagger\varphi W^i_{\mu\nu} W^{\mu\nu i}$$
$$\mathcal{O}_{\varphi WB} = \varphi^\dagger \tau^i \varphi W^i_{\mu\nu} B^{\mu\nu}$$

dimension 8

$$\mathcal{O}_{S,0} = \left[(D_\mu\Phi)^\dagger D_\nu\Phi\right] \times \left[(D^\mu\Phi)^\dagger D^\nu\Phi\right]$$
$$\mathcal{O}_{S,1} = \left[(D_\mu\Phi)^\dagger D^\mu\Phi\right] \times \left[(D_\nu\Phi)^\dagger D^\nu\Phi\right]$$
$$\mathcal{O}_{S,2} = \left[(D_\mu\Phi)^\dagger D_\nu\Phi\right] \times \left[(D^\nu\Phi)^\dagger D^\mu\Phi\right]$$
$$\mathcal{O}_{M,0} = \mathrm{Tr}\left[\hat{W}_{\mu\nu}\hat{W}^{\mu\nu}\right] \times \left[(D_\beta\Phi)^\dagger D^\beta\Phi\right]$$
$$\mathcal{O}_{M,1} = \mathrm{Tr}\left[\hat{W}_{\mu\nu}\hat{W}^{\nu\beta}\right] \times \left[(D_\beta\Phi)^\dagger D^\mu\Phi\right]$$
$$\mathcal{O}_{M,7} = \left[(D_\mu\Phi)^\dagger \hat{W}_{\beta\nu} D^\nu\Phi\right]$$
$$\mathcal{O}_{T,0} = \mathrm{Tr}\left[\hat{W}_{\mu\nu}\hat{W}^{\mu\nu}\right] \times \mathrm{Tr}\left[\hat{W}_{\alpha\beta}\hat{W}^{\alpha\beta}\right]$$
$$\mathcal{O}_{T,1} = \mathrm{Tr}\left[\hat{W}_{\alpha\nu}\hat{W}^{\mu\beta}\right] \times \mathrm{Tr}\left[\hat{W}_{\mu\beta}\hat{W}^{\alpha\nu}\right]$$
$$\mathcal{O}_{T,2} = \mathrm{Tr}\left[\hat{W}_{\alpha\mu}\hat{W}^{\mu\beta}\right] \times \mathrm{Tr}\left[\hat{W}_{\beta\nu}\hat{W}^{\nu\alpha}\right]$$

Same-sign WW with hadronic tau

EFT interpretation

Wilson coefficient		68% CL interval(s) Expected	Observed	95% CL interval Expected	Observed
dim-6	$c_{ll}^{(1)}$	$[-12.9, -8.03] \cup [-2.95, 1.91]$	$[-11.6, 0.045]$	$[-14.6, 3.53]$	$[-13.5, 2.11]$
	$c_{qq}^{(1)}$	$[-0.501, 0.576]$	$[-0.341, 0.416]$	$[-0.742, 0.818]$	$[-0.605, 0.681]$
	c_W	$[-0.681, 0.669]$	$[-0.513, 0.481]$	$[-0.987, 0.974]$	$[-0.842, 0.818]$
	c_{HW}	$[-7.00, 6.09]$	$[-5.48, 4.31]$	$[-9.99, 9.05]$	$[-8.68, 7.60]$
	c_{HWB}	$[-41.7, 69.6]$	$[30.7, 89.2]$	$[-66.6, 96.4]$	$[-49.7, 110]$
	$c_{H\Box}$	$[-16.6, 18.1]$	$[-12.0, 14.0]$	$[-24.7, 26.3]$	$[-20.9, 22.7]$
	c_{HD}	$[-24.6, 34.7]$	$[-15.3, 31.5]$	$[-38.2, 48.8]$	$[-31.4, 45.5]$
	$c_{Hl}^{(1)}$	$[-28.8, 29.9]$	$[-38.2, 39.5]$	$[-49.4, 49.7]$	$[-69.3, 68.3]$
	$c_{Hl}^{(3)}$	$[-1.43, 2.23] \cup [5.88, 9.54]$	$[-0.045, 8.58]$	$[-2.64, 10.8]$	$[-1.59, 9.94]$
	$c_{Hq}^{(1)}$	$[-4.53, 4.42]$	$[-3.27, 3.44]$	$[-6.56, 6.44]$	$[-5.55, 5.60]$
	$c_{Hq}^{(3)}$	$[-2.39, 1.37]$	$[-1.88, 0.705]$	$[-3.24, 2.16]$	$[-2.82, 1.61]$
dim-8	f_{T0}	$[-1.02, 1.08]$	$[-0.774, 0.842]$	$[-1.52, 1.58]$	$[-1.32, 1.38]$
	f_{T1}	$[-0.426, 0.480]$	$[-0.319, 0.381]$	$[-0.640, 0.695]$	$[-0.552, 0.613]$
	f_{T2}	$[-1.15, 1.37]$	$[-0.851, 1.12]$	$[-1.75, 1.98]$	$[-1.51, 1.76]$
	f_{M0}	$[-9.89, 9.74]$	$[-8.07, 7.70]$	$[-14.6, 14.5]$	$[-13.1, 12.8]$
	f_{M1}	$[-12.5, 13.3]$	$[-9.54, 11.15]$	$[-18.7, 19.6]$	$[-16.4, 17.7]$
	f_{M7}	$[-20.3, 19.2]$	$[-17.6, 15.3]$	$[-29.9, 28.8]$	$[-27.6, 25.8]$
	f_{S0}	$[-11.6, 12.0]$	$[-9.60, 9.82]$	$[-17.4, 17.9]$	$[-15.9, 16.1]$
	f_{S1}	$[-37.4, 38.8]$	$[-40.9, 41.3]$	$[-57.2, 58.6]$	$[-60.9, 61.8]$
	f_{S2}	$[-37.4, 38.8]$	$[-40.9, 41.3]$	$[-57.2, 58.6]$	$[-60.9, 61.8]$

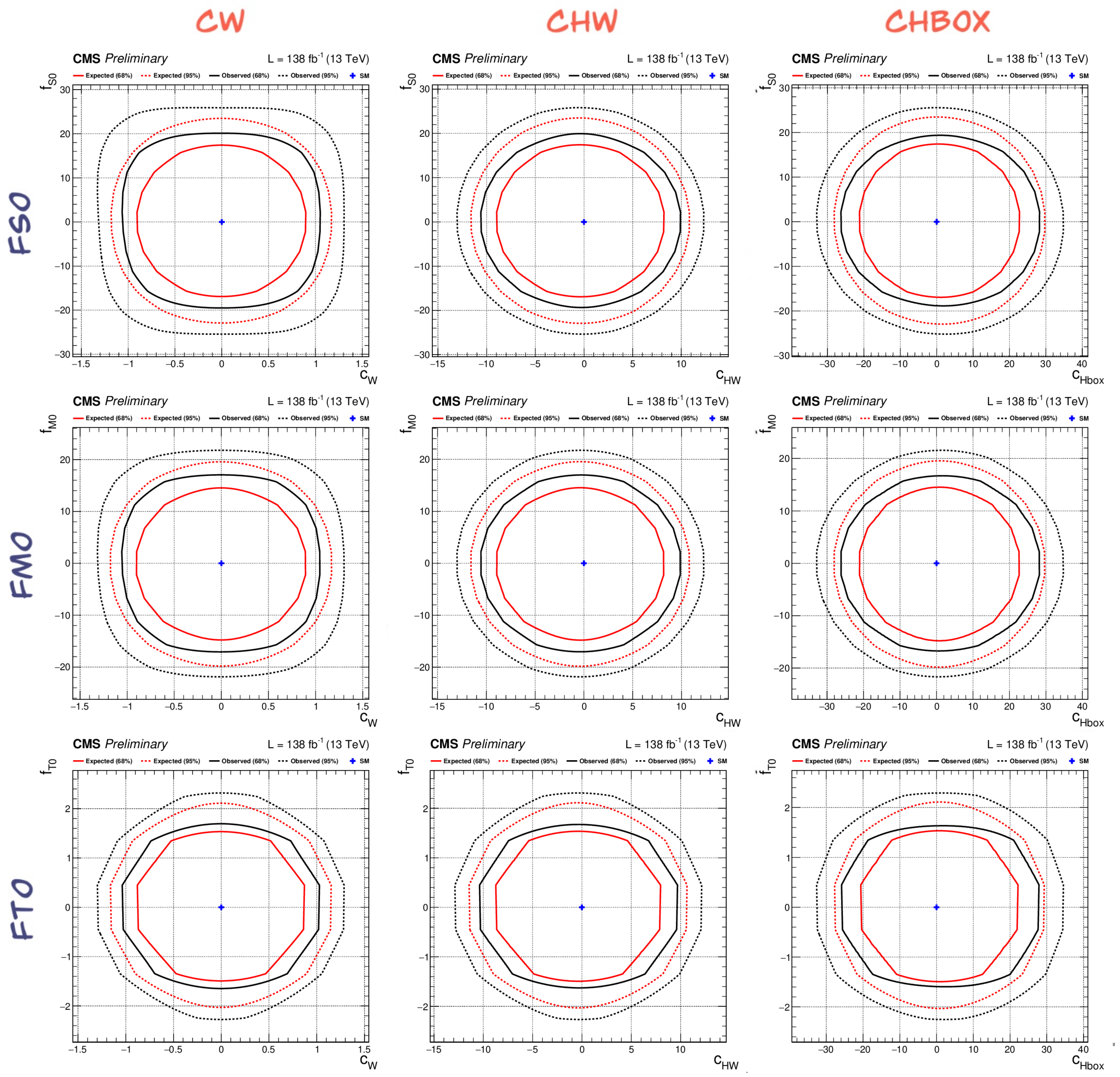

Summary

- Many analyses performed with full Run2 datasets and more to come
- The exploration of Effective Field Theory interpretations is gaining importance in VBS field $\longrightarrow$ Recent studies shown a high sensitivity to dim6 EFT operators and this would allow VBS processes to be integrated into the landscape of global EFT interpretations

What about Run3?

VBS are rare processes, Run3 has started relatively recently and some time is required to carry out precision measurements. Hope for results to come soon!

Backup

Opposite-sign WW VBS

Uncertainties and yields

Uncertainty source	Value
QCD-induced W^+W^- normalization	5.3%
$t\bar{t}$ scale variation	5.1%
VBS signal scale variation	5.0%
$t\bar{t}$ normalization	4.9%
b tagging	3.5%
Trigger corrections	3.3%
DY normalization	2.9%
Jet energy scale + resolution	2.6%
Unclustered p_T^{miss}	2.4%
QCD-induced W^+W^- scale variation	2.1%
Integrated luminosity	2.0%
Muon efficiency	2.0%
Pileup	1.8%
Electron efficiency	1.5%
Underlying event	1.3%
Parton shower	1.0%
Other	$<$1%
Total systematic uncertainty	13.1%
Total statistical uncertainty	14.9%
Total uncertainty	19.8%

Process	SR eμ $Z_{\ell\ell} < 1$	SR eμ $Z_{\ell\ell} > 1$	SR ee - $\mu\mu$ $Z_{\ell\ell} < 1$	SR ee - $\mu\mu$ $Z_{\ell\ell} > 1$
DATA	2441	2192	1606	1667
Signal + background	2396.8 ± 98.5	2239.6 ± 106.0	1590.4 ± 49.4	1660.5 ± 43.6
Signal	169.1 ± 20.2	69.9 ± 8.4	98.0 ± 6.5	38.3 ± 2.5
Background	2227.7 ± 96.4	2169.7 ± 105.6	1492.4 ± 48.9	1622.1 ± 43.5
$t\bar{t}$ + tW	1629.4 ± 71.4	1452.5 ± 69.5	767.8 ± 14.5	642.5 ± 13.2
WW (QCD)	327.0 ± 61.6	409.3 ± 77.3	111.1 ± 16.6	121.5 ± 17.3
Nonprompt	107.0 ± 18.4	109.9 ± 16.4	30.0 ± 4.9	32.0 ± 4.2
DY no PU jets	—	—	259.5 ± 27.3	408.3 ± 17.1
DY + 1 PU jets	—	—	222.7 ± 33.3	337.4 ± 32.9
DY$\tau^+\tau^-$	69.2 ± 4.6	102.0 ± 5.8	—	—
Multiboson	67.7 ± 6.6	75.6 ± 7.3	60.9 ± 3.8	60.1 ± 4.8
Zjj	1.0 ± 0.2	0.4 ± 0.0	40.5 ± 4.2	20.3 ± 1.3
Higgs	26.6 ± 1.5	20.1 ± 1.0	—	—

EWK production of $W\gamma$ +2jets

Differential cross section

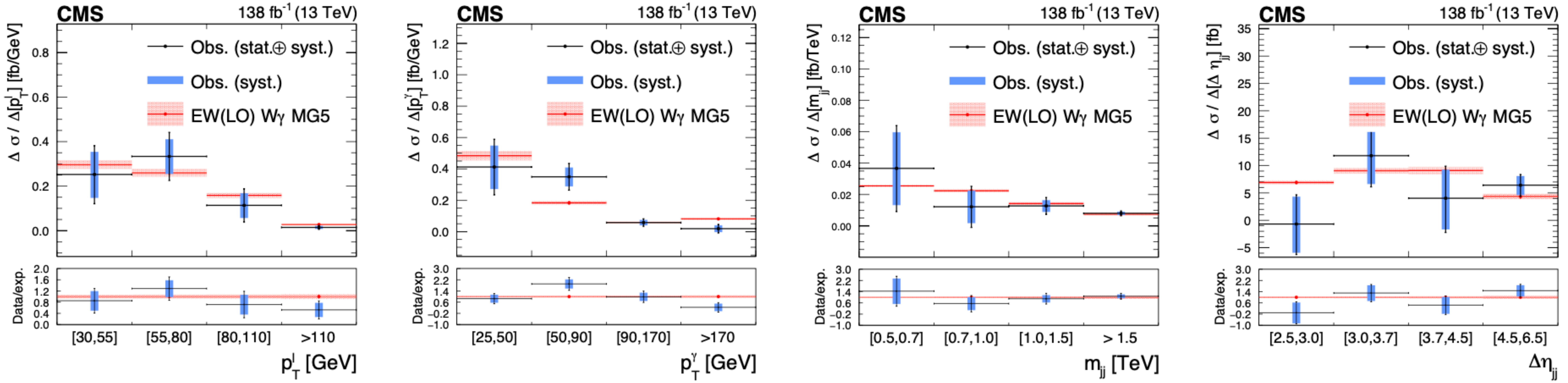

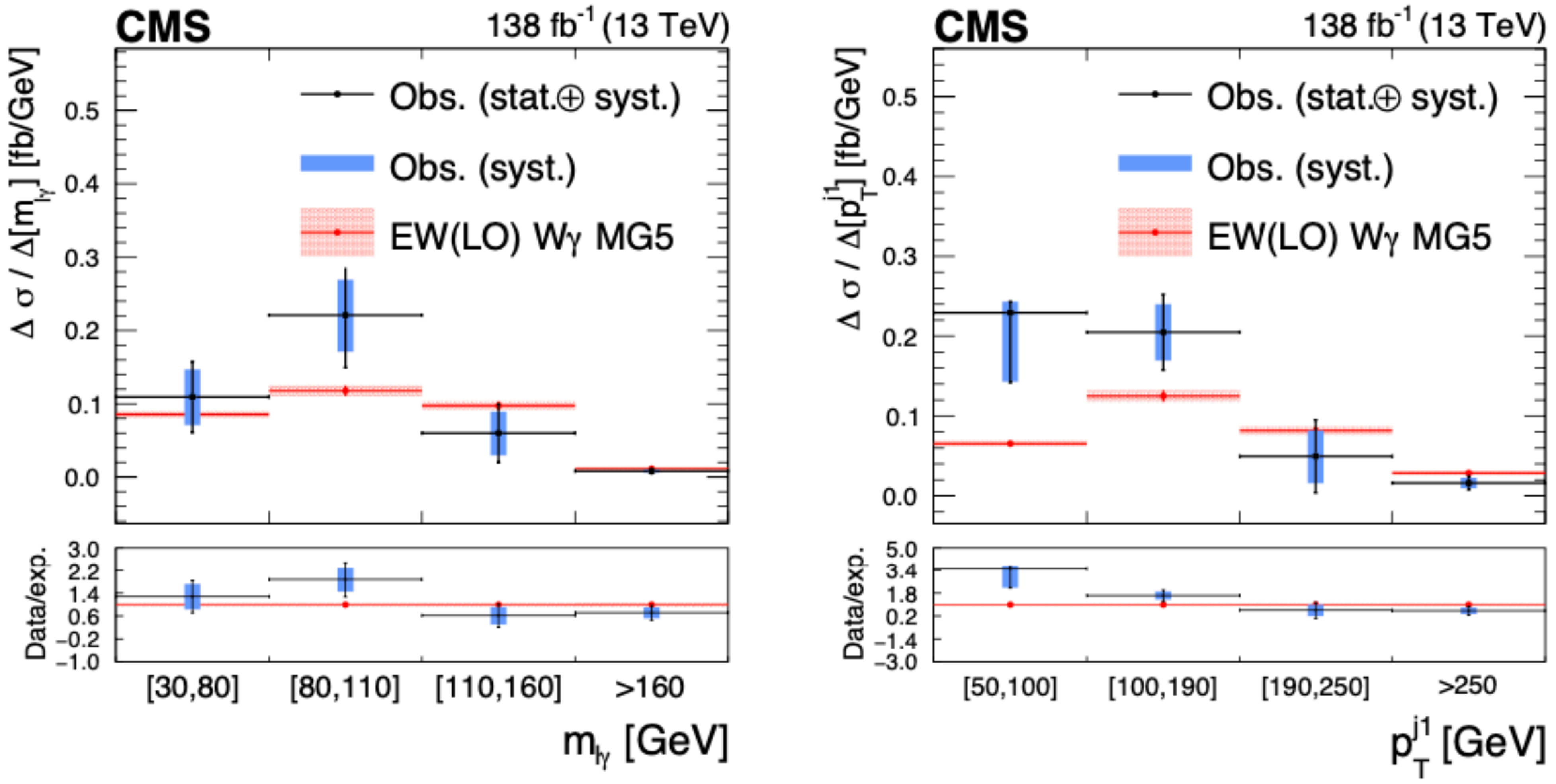

	Barrel	Endcap
EW $W\gamma$ inside fiducial region	316 ± 16	90.2 ± 5.5
EW $W\gamma$ outside fiducial region	64.7 ± 2.0	20.4 ± 1.0
QCD $W\gamma$	1301 ± 28	362 ± 13
top, VV, $Z\gamma$	402 ± 14	93.3 ± 7.2
Nonprompt photon	434 ± 13	120.2 ± 5.7
Nonprompt muon	134 ± 27	45 ± 11
Nonprompt electron	189 ± 20	86 ± 13
Nonprompt photon, nonprompt muon	43.0 ± 7.0	14.6 ± 3.4
Nonprompt photon, nonprompt electron	75.5 ± 5.5	25.0 ± 2.0
Total prediction	2960 ± 43	856 ± 21
Data	2959 ± 57	849 ± 32

EWK production of $W\gamma$ +2jets

Discrimination of prompt and non-prompt photons

Estimate of fake photons rate is done knowing fake photons fraction.

- prompt photon template and the fake photon template are fit to the data template to get the fake fraction for different photon pT bins
- $\sigma\eta\eta < 0.01015$ (0.0272) in barrel (endcap)*

- One loose muon and no other leptons in muon channel,or one veto electron other leptons in electron channel
- HLT pass
- missing ET>30 GeV
- W transverse mass>30 GeV
- $\Delta R_{l\gamma}$ >0.5
- $p_T^{lep} > 30$ GeV, $|\eta^{lep}| < 2.4$ (2.5) muon(ele)
- 25 GeV $< p_T^{\gamma} < 4000$ GeV, $|\eta^{\gamma}| < 1.4442$ (barrel), $1.566 < |\eta^{\gamma}| < 2.5$ (endcap)
- $|M_{l\gamma} - M_Z| > 10$ (ele)
- Photon pixelseed veto

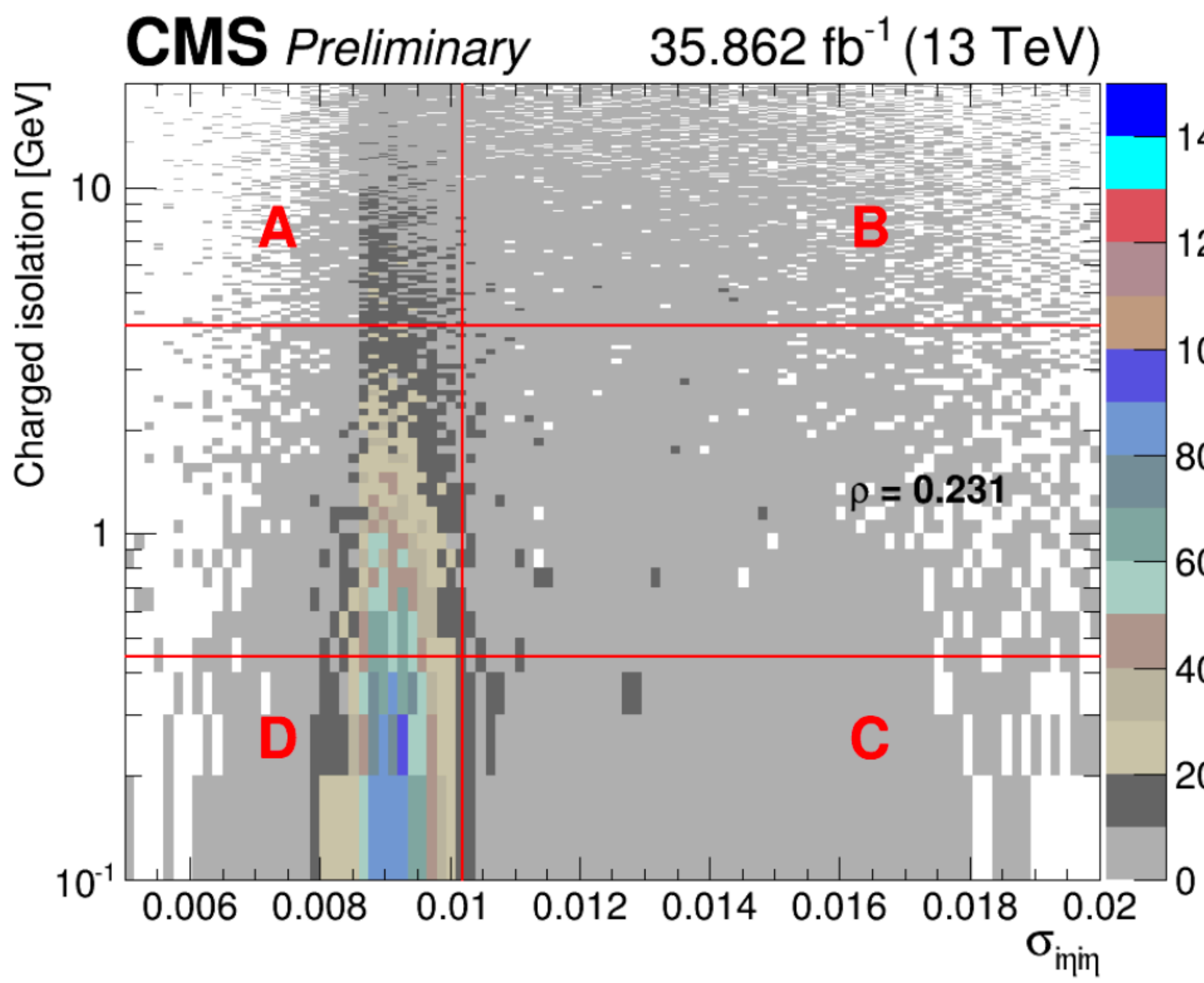

2D distribution of charge isolation and $\sigma\eta\eta$ of photons (D is the good photon region), in other regions objects don't meet requirements for charge isolation and $\sigma\eta\eta$

* energy-weighted spread within the 5×5 crystal matrix centered on the crystal with the largest energy deposit in the supercluster

Same-sign WW with hadronic tau

Non-prompt background estimate

Hadronically decaying taus are reconstructed with hadrons-plus-strips algorithm and identified with DeepTau algorithm based on DNN models, and is capable of discriminating taus from jets, electron and muons using three different classifiers

Region	1 ℓ, 1 τ_h, no additional "loose" ℓ		
	same-sign (ℓ, τ_h)	$p_T^{miss} > 50$ GeV	additional requirements
SR	✓	×	$M_{jj} > 500$ GeV
Nonprompt CR	✓	×	
$t\bar{t}$ CR	×	✓	b-tagged jet ("medium")
OS CR	×	✓	b-tagged jet veto ("loose")
QCD-enriched CR	1 "loose" e, μ, or τ_h, no add. leptons, $p_T^{miss} \leq 50$ GeV, $M_T(\ell, p_T^{miss}) < 50$ GeV		

Non-prompt yield estimated from data CRs by pass-fail method.

- QCD-enriched region (data jet-based trigger) is used to perform the first step of estimate, disjoint from other CRs and SR
- Non prompt region validates the bkg estimate.

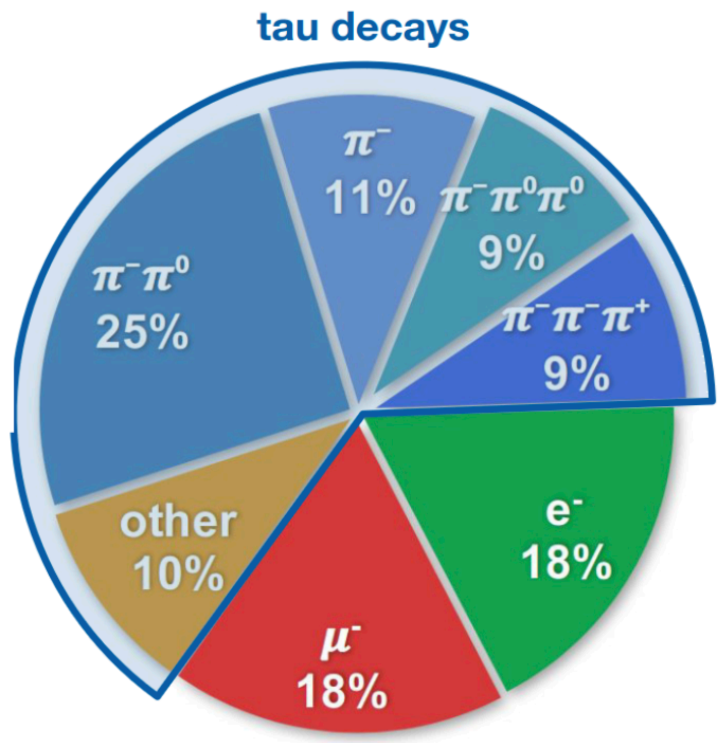

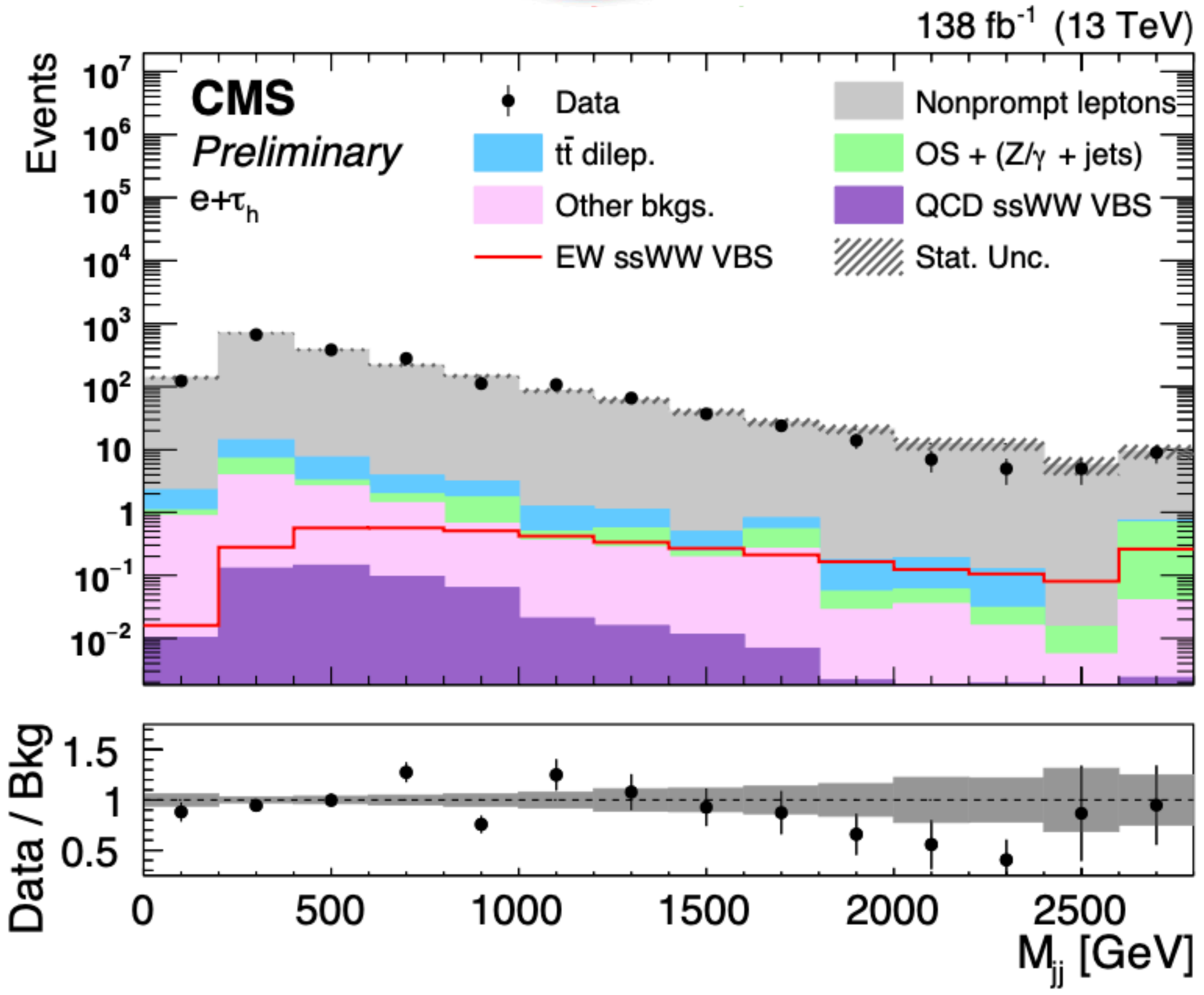

Same-sign WW with hadronic tau

DNN variables and uncertainties

Input variable	SM DNN	dim-6 DNN	dim-8 DNN
$\tau_h\ p_T$	✓	✓	✓
$\ell\ p_T$	✓	✓	✓
$\tau_h\ \eta$		✓	
$\ell\ \eta$		✓	
leading VBS jet p_T	✓	✓	✓
subleading VBS jet p_T	✓	✓	✓
leading VBS jet mass		✓	✓
subleading VBS jet mass		✓	✓
VBS jet pair $\Delta\phi$		✓	
M_{jj}	✓	✓	
M_{1T}	✓	✓	✓
M_{o1}	✓	✓	✓
$M_T(\tau_h, \vec{p}_T^{\,miss})$			✓
$M_T(\ell, \vec{p}_T^{\,miss})$	✓	✓	✓
$M_T(\ell, \tau_h, \vec{p}_T^{\,miss})$			✓
$p_T^{rel}(\ell, j_1)$		✓	
$p_T^{rel}(\ell, j_2)$		✓	
$p_T^{rel}(\tau_h, j_1)$		✓	
$p_T^{rel}(\tau_h, j_2)$		✓	
$\Delta\phi(\ell, j_1)$		✓	
$\Delta\phi(\ell, j_2)$		✓	
$\Delta\phi(\tau_h, j_1)$		✓	
$\Delta\phi(\tau_h, j_2)$		✓	
$p_{T,\text{leading}\ \tau_h\ \text{track}}/p_{T,\tau_h}$	✓	✓	
Zeppenfeld variable		✓	

Uncertainty source	$+\Delta\mu$	$-\Delta\mu$
Theory (PDF, QCD-scale, ISR, and FSR)	+0.157	−0.099
Non-prompt estimation	+0.136	−0.125
$t\bar{t}$ normalization	+0.051	−0.023
Prefiring	+0.105	−0.059
Luminosity	+0.079	−0.092
b-tagging and mistagging	+0.007	−0.004
Jet energy scale and resolution, Pile-up jet ID	+0.079	−0.097
Pileup	+0.152	−0.162
LO-to-NLO VBS corrections	+0.043	−0.025
Unclustered energy	+0.003	−0.010
Hadronic tau energy scale and DEEPTAU	+0.154	−0.152
Charge misidentification	+0.005	−0.010
Lepton reconstruction, identification, and isolation	+0.005	−0.024
MC statistical	+0.324	−0.322
Total systematic uncertainty	+0.344	−0.302
Data statistical uncertainty	+0.522	−0.477
Total uncertainty	+0.625	−0.564

Next to Leading Order corrections

Table 1: Summary of higher-order predictions currently available for the ss-WW channel: at fixed order and matched to parton shower. The symbols ✓, ✓*, and X means that the corresponding predictions are available, in the VBS approximation, or not available yet.

Order	$\mathcal{O}(\alpha^7)$	$\mathcal{O}(\alpha_s\alpha^6)$	$\mathcal{O}(\alpha_s{}^2\alpha^5)$	$\mathcal{O}(\alpha_s{}^3\alpha^4)$
NLO	✓	✓	✓	✓
NLO+PS	✓	✓*	X	✓

Table 7: Summary of higher-order predictions currently available for the os-WW channel: at fixed order and matched to parton shower. The symbols ✓, ✓*, and X means that the corresponding predictions are available, in the VBS approximation, or not yet.

Order	$\mathcal{O}(\alpha^7)$	$\mathcal{O}(\alpha_s\alpha^6)$	$\mathcal{O}(\alpha_s{}^2\alpha^5)$	$\mathcal{O}(\alpha_s{}^3\alpha^4)$
NLO	X	✓*	X	✓
NLO+PS	X	✓*	X	✓

Table 3: Summary of higher-order predictions currently available for the WZ channel: at fixed order and matched to parton shower. The symbols ✓, ✓*, and X means that the corresponding predictions are available, in the VBS approximation, or not yet.

Order	$\mathcal{O}(\alpha^7)$	$\mathcal{O}(\alpha_s\alpha^6)$	$\mathcal{O}(\alpha_s{}^2\alpha^5)$	$\mathcal{O}(\alpha_s{}^3\alpha^4)$
NLO	✓	✓	X	✓
NLO+PS	X	✓*	X	✓

Table 5: Summary of higher-order predictions currently available for the ZZ channel: at fixed order and matched to parton shower. The symbols ✓, ✓*, and X means that the corresponding predictions are available, in the VBS approximation, or not yet.

Order	$\mathcal{O}(\alpha^7)$	$\mathcal{O}(\alpha_s\alpha^6)$	$\mathcal{O}(\alpha_s{}^2\alpha^5)$	$\mathcal{O}(\alpha_s{}^3\alpha^4)$
NLO	✓	✓	X	✓
NLO+PS	X	✓*	X	✓

WV semi-leptonic

- First evidence for EW production of WV+2jets (V = W,Z) in semi-leptonic channel
- To maximize the efficiency for the signal, different selection requirements are applied depending on jet pT.Two categories of events, based on recontruction of hadronically decaying V: resolved (2 distinct jets with dijet mass ~Vmass) or boosted (1 large-radius jet)
- Multivariate ML discriminators optimized to separate signal and bkgs

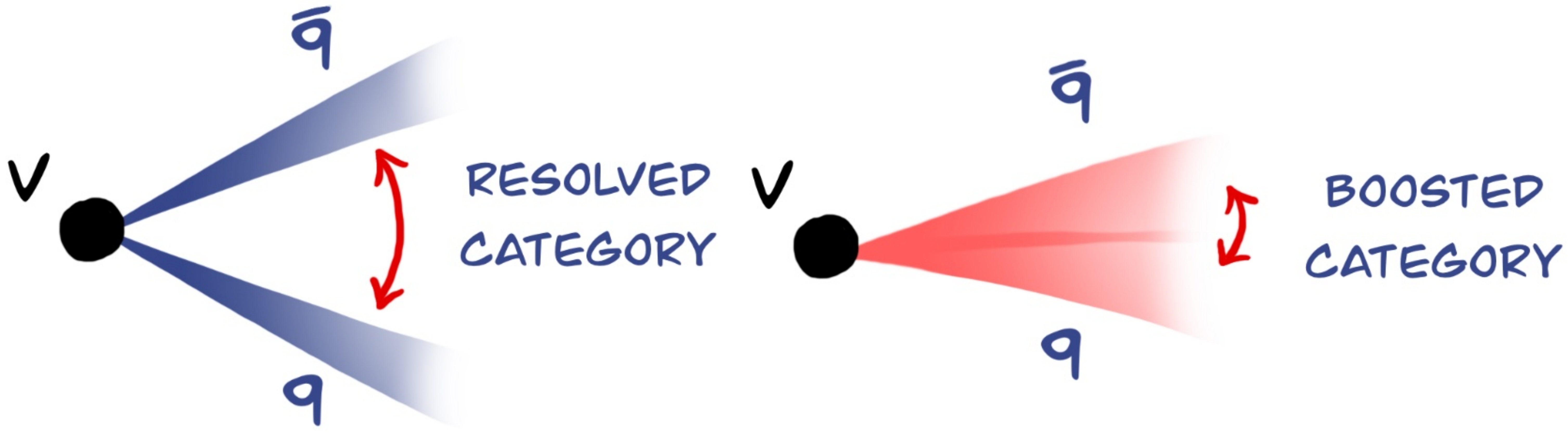

WV semi-leptonic

- Measurement of purely EW WV signal strenght ($\mu_{QCD} = 1$) and EWK+QCD WV signal strenght (EWK/QCD ratio fixed to SM) in a fiducial phase space region.

Signal	$\mu = \sigma_{OBS}/\sigma_{SM}$	Cross Section [pb]
EWK WV	$0.85 \pm 0.12(\text{stat})^{+0.19}_{-0.17}(\text{syst})$	$1.90^{+0.53}_{-0.46}$
EWK+QCD WV	$0.97 \pm 0.06(\text{stat})^{+0.19}_{-0.21}(\text{syst})$	$16.4^{+3.5}_{-2.8}$

Significance 4.4 σ (5.1 σ exp.)

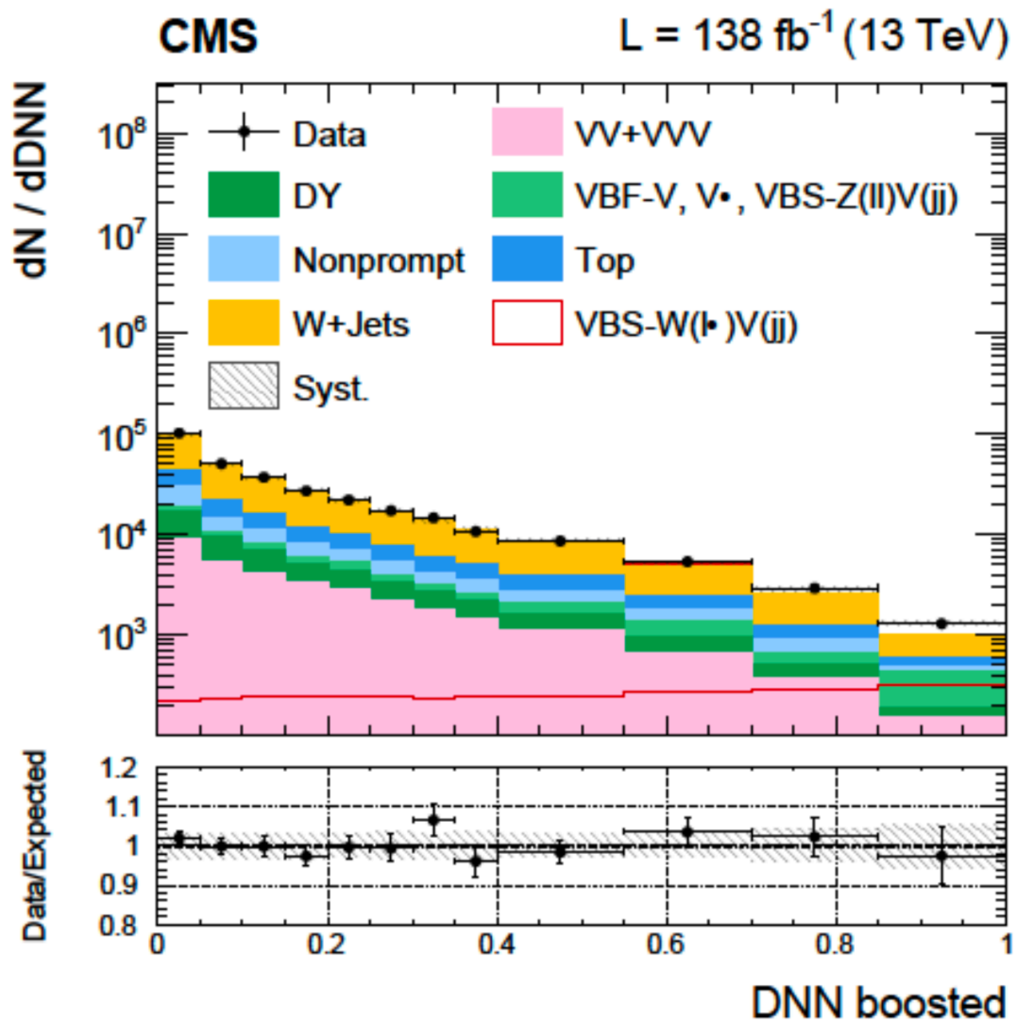

- Simultaneous EW and QCD WV production fit: signal strenghts of two components are left as free independent parameters.

Agreement with SM predictions within 68% CL

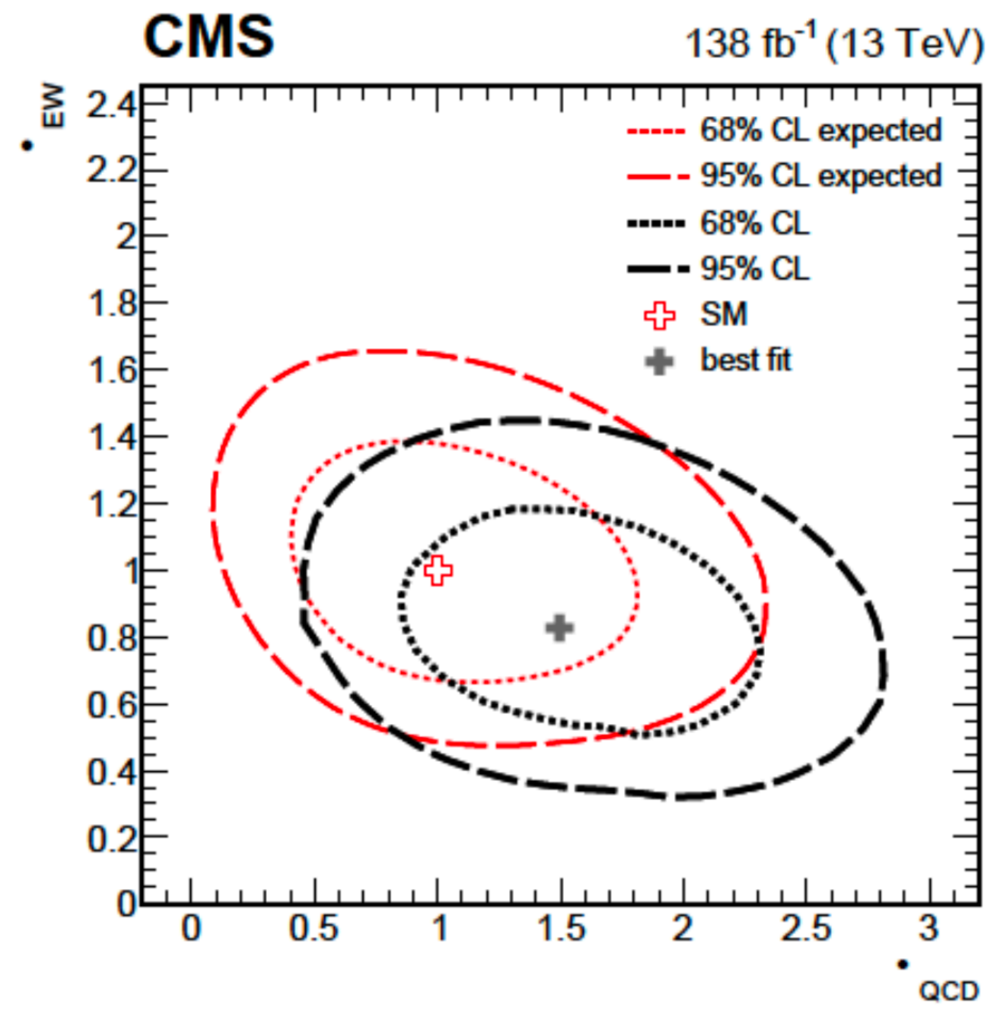

Summary of other results

ZZ to 4L + 2jets

	Perturbative order	SM σ (fb)	Measured σ (fb)
		ZZjj inclusive	
EW	LO	0.275 ± 0.021	$0.33^{+0.11}_{-0.10}\,(\text{stat})^{+0.04}_{-0.03}\,(\text{syst})$
	NLO QCD	0.278 ± 0.017	
	NLO EW	$0.242^{+0.015}_{-0.013}$	
EW+QCD		5.35 ± 0.51	$5.29^{+0.31}_{-0.30}\,(\text{stat}) \pm 0.47\,(\text{syst})$
		VBS-enriched (loose)	
EW	LO	0.186 ± 0.015	$0.180^{+0.070}_{-0.060}\,(\text{stat})^{+0.021}_{-0.012}\,(\text{syst})$
	NLO QCD	0.197 ± 0.013	
EW+QCD		1.21 ± 0.09	$1.00^{+0.12}_{-0.11}\,(\text{stat}) \pm 0.07\,(\text{syst})$
		VBS-enriched (tight)	
EW	LO	0.104 ± 0.008	$0.09^{+0.04}_{-0.03}\,(\text{stat}) \pm 0.02\,(\text{syst})$
	NLO QCD	0.108 ± 0.007	
EW+QCD		0.221 ± 0.014	$0.20^{+0.05}_{-0.04}\,(\text{stat}) \pm 0.02\,(\text{syst})$

$-0.24 < f_{T0}/\Lambda^4 < 0.22$

$-0.31 < f_{T1}/\Lambda^4 < 0.31$

$-0.63 < f_{T2}/\Lambda^4 < 0.59$

$-0.43 < f_{T8}/\Lambda^4 < 0.43$

$-0.92 < f_{T9}/\Lambda^4 < 0.92$

Most stringent limits to date on FT8 and FT9 dim-8 operators.

Polarized ssWW

WW CoM frame

Process	$\sigma\mathcal{B}$ (fb)	Theoretical prediction (fb)
$W^\pm_L W^\pm_L$	$0.32^{+0.42}_{-0.40}$	0.44 ± 0.05
$W^\pm_X W^\pm_T$	$3.06^{+0.51}_{-0.48}$	3.13 ± 0.35
$W^\pm_L W^\pm_X$	$1.20^{+0.56}_{-0.53}$	1.63 ± 0.18
$W^\pm_T W^\pm_T$	$2.11^{+0.49}_{-0.47}$	1.94 ± 0.21

p-p CoM frame

Process	$\sigma\mathcal{B}$ (fb)	Theoretical prediction (fb)
$W^\pm_L W^\pm_L$	$0.24^{+0.40}_{-0.37}$	0.28 ± 0.03
$W^\pm_X W^\pm_T$	$3.25^{+0.50}_{-0.48}$	3.32 ± 0.37
$W^\pm_L W^\pm_X$	$1.40^{+0.60}_{-0.57}$	1.71 ± 0.19
$W^\pm_T W^\pm_T$	$2.03^{+0.51}_{-0.50}$	1.89 ± 0.21

Observed (expected) CL@95% upper limit on xsec for L-polarized ssWW: 1.17 (0.88) fb (WW CoM frame)

EWK production for ssWW (at least one W longitudinally polarized) lead to observed (expected) significance of 2.3 (3.1) σ.